THESIS FOR THE DEGREE OF DOCTOR OF TECHNOLOGY

Early Hydration of Portland Cement

- An Infrared Spectroscopy Perspective Complemented by Calorimetry and Scanning Electron Microscopy

E. Rikard Ylmén

Department of Chemical and Biological Engineering
CHALMERS UNIVERSITY OF TECHNOLOGY
Gothenburg, Sweden 2013

Early Hydration of Portland Cement
- An Infrared Spectroscopy Perspective Complemented by Calorimetry and Scanning Electron Microscopy
E. RIKARD YLMÉN
ISBN 978-91-7385-853-3

© E. RIKARD YLMÉN, 2013.

Doktorsavhandlingar vid Chalmers tekniska högskola
Ny serie nr 3534
ISSN 0346-718X

Department of Chemical and Biological Engineering
Chalmers University of Technology
SE-412 96 Gothenburg
Sweden
Telephone + 46 (0)31-772 1000

Cover: Crystal structure of ettringite, see page 15

Chalmers Reproservice
Gothenburg, Sweden 2013

Early Hydration of Portland Cement
- An Infrared Spectroscopy Perspective Complemented by Calorimetry and Scanning Electron Microscopy
E. RIKARD YLMÉN

Department of Chemical and Biological Engineering

Chalmers University of Technology

ABSTRACT

More than 3 billion tonnes of cement is produced annually worldwide. One tonne of cement results in approximately 0.8 tonnes of CO_2 and requires about 3 GJ of energy if produced by the currently most energy-efficient methods. The production of cement is responsible for approximately 7 % of the total CO_2 emissions caused by man. To compensate for high energy consumption and CO_2 emission, thus making the utilization of concrete more sustainable, several strategies can be used. Regardless of the approach used to construct the ultimate sustainable concrete, tools to evaluate the effects of the efforts are needed. In this work methodologies whereby Fourier Transform Infrared (FTIR) spectroscopy can be made use of, both *in situ* and *ex situ*, have been proposed and validated by means of complementary techniques including scanning electron microscopy, Vicat, and isothermal calorimetry. The FTIR techniques were proven to offer powerful tools for monitoring the complex chemical reactions taking place during the first day of Portland cement hydration. Sulfate transformations and interplay between hydration and carbonation are two examples of cement chemistry which has been addressed. The complementarity of isothermal calorimetry and *in situ* FTIR was demonstrated in particular. Usefulness of the latter for the study of the first stages of cement hydration emerges. The novel approach offers detailed chemical information which allows for the evaluation of additives regarding the nature of their effects on the overall cement performance. In this spirit, the impacts of colloidal nano-silica (CNS), sodium hydroxide and calcium chloride were described. This work hopes to contribute a chemical analytic tool to serve in the quest for sustainability of built environment with regard to energy and materials.

Keywords: cement, hydration, infrared spectroscopy, FTIR, nano-silica, freeze-drying, carbonation, calorimetry, SEM

LIST OF PUBLICATIONS

This thesis is based on the work contained in the following papers, referred to by Roman numerals in the text:

I. Ylmén R., Larsson K., Jäglid U., Panas I., Steenari B-M., *DR-FTIR method for the study of early hydration of cement*, Conference Proceedings for "SCC 2008: Challenges and Barriers to Application", Chicago, Illinois, November 10–12 (2008).

II. Ylmén R., Jäglid U., Steenari B-M., Panas I., *Early hydration and setting of Portland cement monitored by IR, SEM and Vicat techniques*, Cement and Concrete Research 39 (2009) 433–439.

III. R. Ylmén, L. Wadsö, I. Panas, *Insights into Early Hydration of Portland Limestone Cement from Infrared Spectroscopy and Isothermal Calorimetry*, Cement and Concrete Research 40 (2010) 1541–1546.

IV. Ylmén R., Jäglid U., *Carbonation of Portland Cement Studied by Diffuse Reflection Fourier Transform Infrared Spectroscopy*, International Journal of Concrete Structures and Materials, accepted 4 April 2013, to be published.

V. Ylmén R., Jäglid U., Panas I., *Monitoring early hydration of cement by ex situ and in situ ATR-FTIR - a comparative study*, Manuscript.

Contents

1 Introduction 1

2 Cement Chemistry 4

2.1 Manufacturing of Portland Cement 4

2.2 Cement Chemistry Notation.. 5

2.3 General Hydration Processes of the Main Components of Portland Cement 5

2.3.1 Influence of water on cement 6

2.3.2 Alite 7

2.3.3 Belite 8

2.3.4 Reaction products of alite and belite... 9

2.3.5 Aluminate 12

2.3.6 Ferrite 12

2.3.7 Reaction products of aluminate and ferrite 14

2.4 Calcium Carbonate 16

2.5 Colloidal Nano-Silica in Cement 18

3 Experimental Techniques 19

3.1 Material and Sample Preparation 19

3.2 Fourier Transform Infrared (FTIR) Spectroscopy 19

3.2.1 Motivation 19

3.2.2 Basics... 20

3.2.3 Measuring technique 21

3.2.4 DR-FTIR 23

3.2.5 ATR 23

3.2.6 Transmission FTIR 24

3.3 Vicat 24

3.4 Isothermal Calorimetry 26

3.5 Scanning Electron Microscopy - SEM 27

4 Summary of Papers 29

4.1 Time Resolved Analysis of Cement Hydration by *ex situ* DR-FTIR30

4.1.1 Sampling while hydrating by freeze-drying 30

4.1.2 Complementary observations by SEM, Vicat and *ex situ* DR-FTIR (Paper I and Paper II) 30

4.1.3 Complementary observations by Isothermal Calorimetry and *ex situ* DR-FTIR (Paper III) 33

4.2 Time Resolved Analysis of Cement Hydration by *in situ* ATR-FTIR Spectroscopy 35

4.2.1 Sample preparation for the ATR-FTIR analysis 35

4.2.2 Comparison between *ex situ* FTIR and *in situ* FTIR (Paper V)36

4.3 *In Situ* ATR and Isothermal Calorimetry (Paper V) 37

4.4 Application - Carbonation (Paper IV) 38

4.5 Application - Accelerators (Paper I and Paper V) 40

5 Conclusions and Outlook 45

6 Acknowledgements 47

7 References 48

1 Introduction

Concrete is a widely used building material. It is the second most used substance, only surpassed by water. It is a composite material consisting of cement as binder, sand and stones as aggregates and steel bars as reinforcement. When water is added the cement hardens and binds together the other components.

More than 3 billion tonnes of cement is produced annually worldwide [1]. One tonne of cement results in approximately 0.8 tonnes of CO_2 and requires about 3 GJ of energy if produced by the currently most energy-efficient methods [2]. The production of cement is responsible for approximately 7 % of the total CO_2 emissions caused by man [3]. The energy consumption is hence more than 2500 TWh/year. Yet, this figure only accounts for the production of cement. Neither the energy costs for transportation of the cement and the raw materials nor the energy costs for manufacturing and transportation of aggregates and reinforcement are included. As a reference, the total energy consumption of Sweden is about 400 TWh/year [4].

There are no indications that the amount of cement produced will decrease. From the year 1998 to 2012 the annual cement production increased from 1.5 billion tonnes to 3.4 billion tonnes. A four-fold increase in the annual amount of produced cement to the year 2050 is estimated [5].

The calcium silicates alite (Ca_3SiO_5) and belite (Ca_2SiO_4) are essential to the build-up of strength in hydrated Portland cement. Alite is responsible for short term strength development (days to months) whereas belite displays better long term strength development and performance (months to years). The demand for increasingly shorter setting time and early strength by the building sector has led to an increase in the alite/belite ratio in commercial Portland cement. Belite is formed at temperatures above 800 °C. To transform some of the belite to alite more burned lime, CaO, must be added and the temperature must be raised to above 1400 °C. Consequently more energy is required to produce cement with higher alite/belite ratio.

To compensate for high energy consumption and CO_2 emission, thus making the utilization of concrete more sustainable, several strategies can be used:

- Increase the strength of the concrete, which makes it possible to use less concrete when it is used as a load-bearing element.
- Increase the durability of the concrete, which will prolong the lifetime of the concrete constructions and decrease the need for production of new structures to replace old.
- Ensure that the concrete is properly maintained and repaired when needed.
- Develop methods to re-use concrete, either by crushing it and use it as filler or by making concrete elements that can be taken from old building and be used in the construction of new buildings.

- Add mineral waste that can be used as a reactive component in the cement, for example fly ash from coal power plants, blast furnace slag from iron production or ash from municipal waste burning. Thus the amount of cement is decreased and the waste is used instead of land-fill.
- Making the production and transportation of cement and raw material more energy-efficient.
- Decreasing the alite/belite ratio of the cement and instead accelerating the hydration and early strength of the cement with additives.

Regardless of the approach used to construct the ultimate sustainable concrete, tools to evaluate the effects of the efforts are needed. The performance of the hardened concrete is evaluated by testing macroscopic properties e.g. compressive strength, porosity, fatigue resistance and chemical resistance to various chemicals such as chlorides and organic acids. However, the service life of concrete structures is long, at least a few decades. It is impractical to evaluate new products for such long periods of time. Therefore accelerating conditions are often employed, where the test subjects are exposed to considerably harsher conditions than is expected in real service. The testing period can therefore be substantially shorter, facilitating the transfer of new ideas into application. Another approach is based on the realisation that the macroscopic properties are dictated by the microscopic properties, i.e. the chemical composition and morphology of the microstructure. The macroscopic and microscopic approaches are complementary and are preferably combined.

Given that Portland cement in its present form has existed for 150 years, one would perhaps expect that all aspects of the chemical transformations taking place have been thoroughly studied and completely determined. Indeed, a lot of work has been performed and much of the reactions have been charted. However, controversies regarding the exact nature of the early hydration still persist [2, 6].

The transient physical nature of cement during the first 24 hours presents difficulties for most measuring techniques. The cement starts as powder, which is a solid mixture of several chemical phases more or less crystalline and well-defined. The powder is mixed with water forming a high-viscous, opaque slurry. In this slurry the clinker phases react with the water forming mostly amorphous products. These products can also transform further. As water is reacting and incorporated in the hydration products the slurry will stiffen and solidify. After 24 hours of hydration the result is thus a solid containing amorphous hydration products, unreacted clinker, and unreacted water. Amorphous phases are difficult to characterize. However, the chemistry and morphology of the products are crucially important as they determine the strength of the paste.

The chemistry is further complicated by additives added to the mix. These may comprise accelerators, retarders, plasticisers, fillers and more. External factors such as temperature, mixing procedure and relative humidity are also affecting all the hydration processes. Presently, no single method exists which can follow the hydration process in its entirety and therefore a combination of methods is needed. In this work methodologies whereby Fourier Transform Infrared (FTIR) spectroscopy can be made use of have been proposed and validated. Thus powerful tools focused at the monitoring of chemical reactions taking place during the first day of Portland cement hydration, and complementary to existing techniques, has been developed. They have also been applied to study carbonation of the early hydration products, and the effect of accelerators, i.e. colloidal nano-silica (CNS), sodium hydroxide and calcium chloride.

2 Cement Chemistry

The cement used in this work is Portland limestone cement which is a widely used binder in construction. It is a form of Ordinary Portland Cement (OPC), the most common type of cement around the world. Cement is not a well-defined material since it can contain a variety of chemical compositions and additives. In this chapter an overview of important concepts of cement chemistry is presented.

2.1 Manufacturing of Portland Cement

The manufacturing of OPC can be described as follows [2]: (i) Crushing of a calcareous material (e.g. limestone) and an argillaceous material (e.g. clay or shale), (ii) mixing them together in the right proportions, (iii) transport of the material through a kiln where it is heated to about 1450 ºC and reacts to form clinkers. Finally, these clinkers are ground together with gypsum to produce the final product. Gypsum is added during the grinding process to decrease the reactivity of the cement. The reactions taking place at different temperatures in the kiln are presented in Figure 2.1.

Below 1300 ºC

The most important reactions below 1300 ºC are

- thermal decomposition of calcite to lime (CaO) and CO_2,
- decomposition of clay minerals
- reaction of lime with quartz and clay minerals decomposition products to give belite, aluminate and ferrite.

Only a minor amount of liquid phase is formed at this stage, but this melt has an important effect in promoting reactions. At the end of this stage, the major phases present are belite, lime, aluminate and ferrite. However, the last two may not be identical with the corresponding phases in the final product.

1300-1340 ºC

In the temperature range 1300–1340 ºC clinker formation occur. A melt is formed, mainly from the aluminate and ferrite, and at 1450 ºC some 20–30 % of the mix is liquid. Much of the belite and nearly all the lime react in the presence of the melt to give alite. The material nodulizes, to form the clinker

Cooling

During cooling the liquid crystallizes, giving mainly aluminate and ferrite. In addition, polymorphic transitions of the alite and belite occur

Figure 2.1. Different reactions taking place in the kiln.

2.2 Cement Chemistry Notation

The Ordinary Portland Cement (OPC) ideally consists of four major mineral phases:

Alite Ca_3SiO_5	(50–70 weight%)
Belite Ca_2SiO_4	(15–30 weight%)
Aluminate $Ca_3Al_2O_6$	(5–10 weight%)
Ferrite $Ca_4Al_2Fe_2O_{10}$	(5–15 weight%)

To simplify the formulas used in cement chemistry a special notation is used. It provides a shorter way of writing the chemical formula of oxides of calcium, silicon, and various metals.

In cement chemistry chemical formulae are often expressed as a sum of oxides. Alite will then be written as $3CaO \cdot SiO_2$. Note that this does not mean that the constituent oxides have any separate existence within the structure. According to the cement chemistry notation the oxides are then abbreviated as follows:

$C = CaO$
$S = SiO_2$
$A = Al_2O_3$

$F = Fe_2O_3$
$\bar{S} = SO_3$
$H = H_2O$

Alite is then written as C_3S, belite as C_2S, aluminate as C_3A and ferrite as C_4AF. The formulae of simple oxide phases (like CaO) are usually written in full.

In real cement these phases are not pure. Typical incorporation of foreign ions in the corresponding mineral phases includes:

C_3S / C_2S: Mg^{2+}, Al^{3+}, Fe^{3+}

C_3A: Si^{4+}, Fe^{3+}, Na^{+}, K^{+}

C_4AF: varying Al/Fe ratios

2.3 General Hydration Processes of the Main Components of Portland Cement

The *hydration* of cement denotes the chemical reactions that occur when the cement is mixed with water. The *setting* of cement means stiffening of the cement paste without significant development of compressive strength, and typically occurs within a few hours. This can be measured with a consistency measuring device, such as a Vicat apparatus. The *hardening* means significant development of strength, and is normally a slower process.

2.3.1 Influence of water on cement

Water is essential in cement chemistry. It acts both as a solvent for the clinker ions, as they are transferred from the clinker phase to the reaction products, and as a constituent in the reaction products. The whole process is referred to as *hydration*, meaning incorporation of water, and the products are called *hydrates*, meaning chemical compounds containing water molecules. It should be emphasized that the mineral phases dissolve in solution prior and during the hydration process. The hydration products are therefore more associated with the solved species in the solution than with the individual minerals phases.

Water is a good solvent for charged ions due to its highly polar character and ability to form hydrogen bonds. The hydrogen in water can be substituted with the heavier isotope deuterium to give heavy water, D_2O. Although isotopic substitution usually doesn't change the chemical properties of a molecule, the large difference in mass between hydrogen and deuterium (deuterium being twice as heavy as hydrogen) will result in slightly weaker hydrogen bonds and ability to dissolve ions [7, 8]. This has a large effect on cement hydration. The D_2O has a retarding effect on the rate of hydration of cement. Figure 2.2 illustrates this isotopic effect, seen as a decrease in the hydration rate. Thus, hydrogen bonding and dissolving of ions in water is most likely to be of great importance for the hydration process.

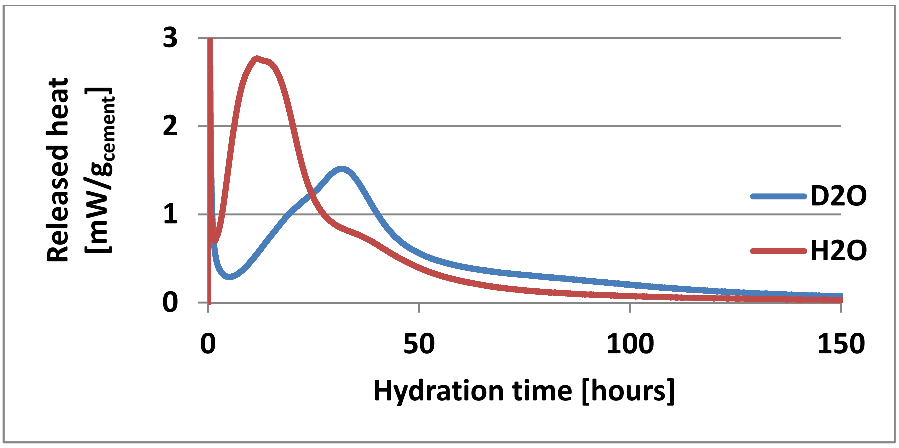

Figure 2.2. Measurements with isothermal calorimetry on Portland limestone cement with water (H_2O) and heavy water (D_2O).

To obtain high strength in cement the mass ratio between water and cement (the w/c ratio) should be near 0.3. However, the workability of cement often requires that the w/c ratio is higher. The amount of water has relatively small effect on the kinetics of the early hydration, as seen in Figure 2.3. Plasticisers can be added to the cement mixture to lower the water demand for a desired workability. They act by separating the cement particles preventing the formation of aggregates trapping water.

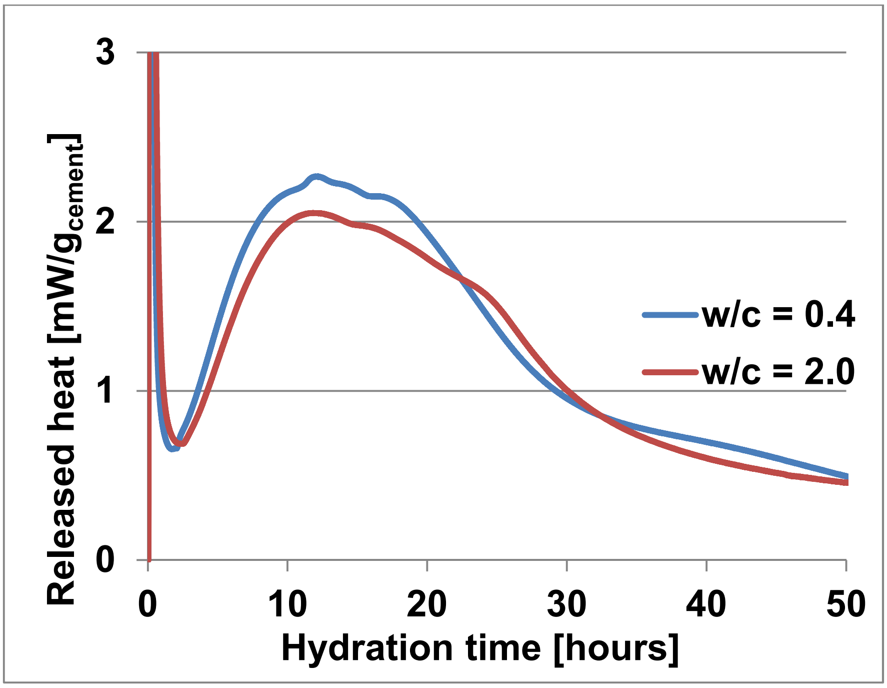

Figure 2.3. Measurements with isothermal calorimetry on Portland limestone cement with different w/c ratios.

2.3.2 Alite

Alite (Ca_3SiO_5, C_3S in cement notation), Figure 2.4, is the most important constituent of all Ordinary Portland Cement clinkers. It reacts relatively quickly with water, and is the most essential of the constituent phases for strength development. At aging up to 28 days it is by far the most important. Alite is formed when belite reacts with CaO at the maximum clinkering temperature of 1400–1500 ºC.

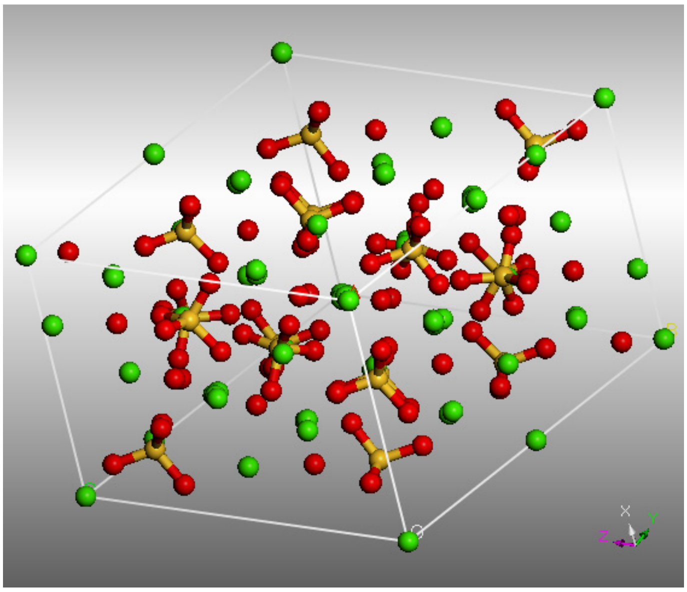

Figure 2.4. Crystal structure of alite showing showing calcium (green), silicon (yellow) and oxygen (red).

2.3.3 Belite

Belite (Ca_2SiO_4, C_2S in cement notation) is normally present wholly or largely as the β polymorph. The mineral name of β-belite is larnite, which is the high temperature crystal structure of belite (Figure 2.5). In order to obtain this structure the clinkers have to be cooled rapidly to avoid the transition from the β polymorph to the γ polymorph; the β polymorph is stable above 500 ºC and the γ polymorph at room temperature. The γ polymorph hydrates very slowly and is therefore undesired as a component in cement. It has a crystal structure similar to olivine ($(Mg,Fe)_2SiO_4$) and are also called calcio-olivine (Figure 2.6)

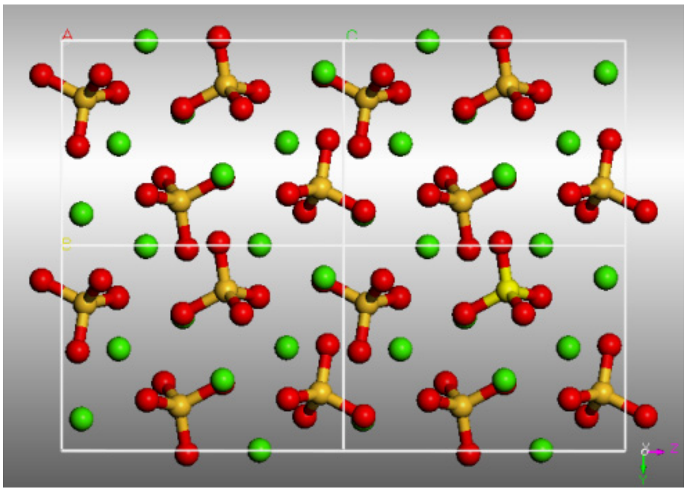

Figure 2.5. Crystal structure of β-belite showing calcium (green), silicon (yellow) and oxygen (red) [9].

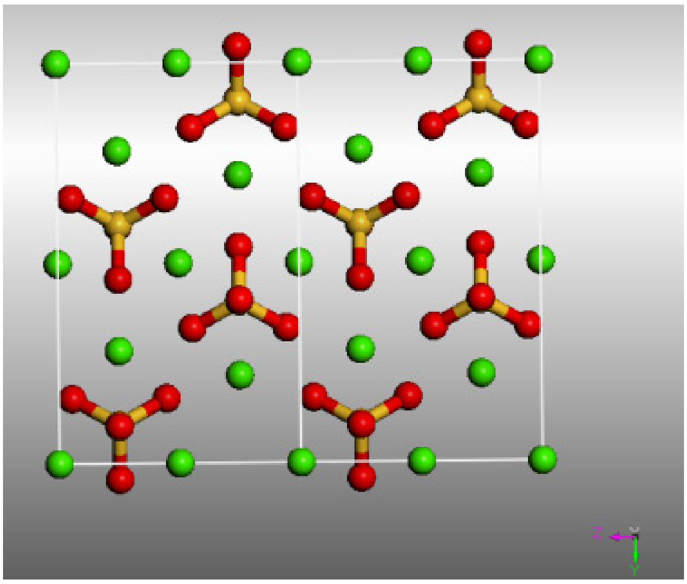

Figure 2.6. Crystal structure of γ-belite showing calcium (green), silicon (yellow) and oxygen (red) [10].

2.3.4 Reaction products of alite and belite

When alite, C_3S, hydrates it forms calcium hydroxide (CH in cement notation) and a solid calcium silicate hydrate that consists of a varying composition of C, S and H, often denoted a C-S-H gel. The C-S-H gel is nearly amorphous and the slashes indicate that the composition of the constituent phases is not stoichiometric (as opposed to writing CSH which implies a one to one correspondence between the constituent phases). The hydration can be written according to reaction (2.1), where x represent the variable amount of water associated to the C-S-H gel.

$$C_3S + (3 - y + x)H \rightarrow C_ySH_x + (3-y)CH \qquad (2.1)$$

The Ca/Si ratio of the C-S-H gel (y in reaction 2.1) varies, but is commonly between 1.5– 2.2 [2].

Belite reacts relatively slowly with water, thus contributing to a less extent to the strength during the first 28 days. However, it contributes substantially to the further increase in strength that occurs at later aging. After about one year, the strength obtained from pure alite and pure belite is about the same under comparable conditions. The hydration products of belite are similar to those of alite, but it is much slower in reacting and less CH is formed.

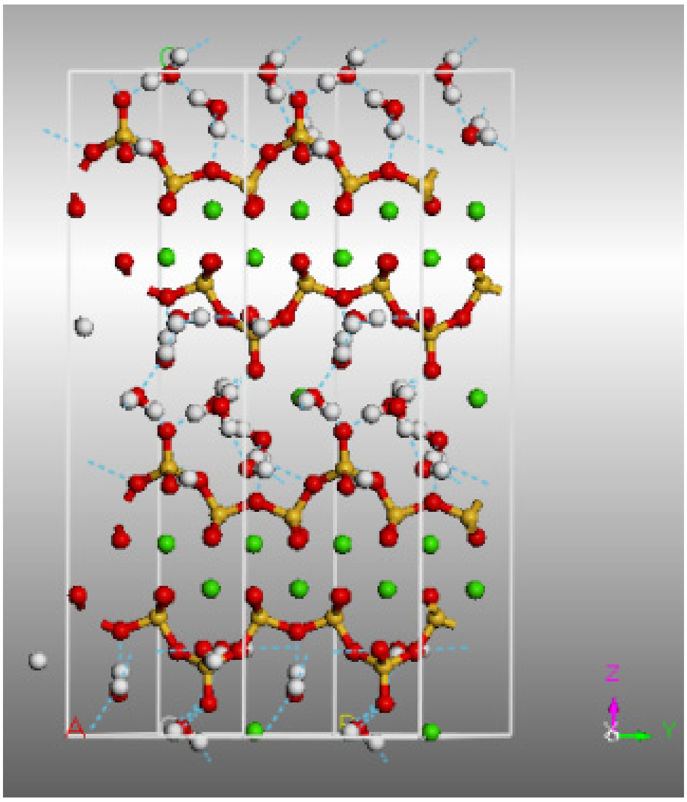

Figure 2.7. Crystal structure of tobermorit-14 Å showing calcium (green), silicon (yellow), oxygen (red), and hydrogen (white) [12].

The actual structure of C-S-H is not known, but it is often compared to tobermorite-14Å and jennite. The silica in both tobermorite and jennite forms infinite chains with a "dreierkette" structure. The chains consist of silica dimers connected by bridging SiO_4 tetrahedrons. The chains are visible in Figure 2.7 and Figure 2.8. During early stages of cement hydration only silica dimers are formed. As the hydration progresses oligomers will form, but even after several years there will be a substantial amount of smaller oligomers, such as pentamers and octamers [2]. Iler [11] noted that the presence of calcium is essential to form silica dimers, since alkaline solutions with only sodium as the positive ion will not contain any dimers.

Calcium has a similar coordination with oxygen in both jennite and tobermorite. Four oxygen atoms form a quadratic flat girdle and then there are oxygen atoms with longer bond distance to calcium above and below the girdle resulting in an octahedral structure.

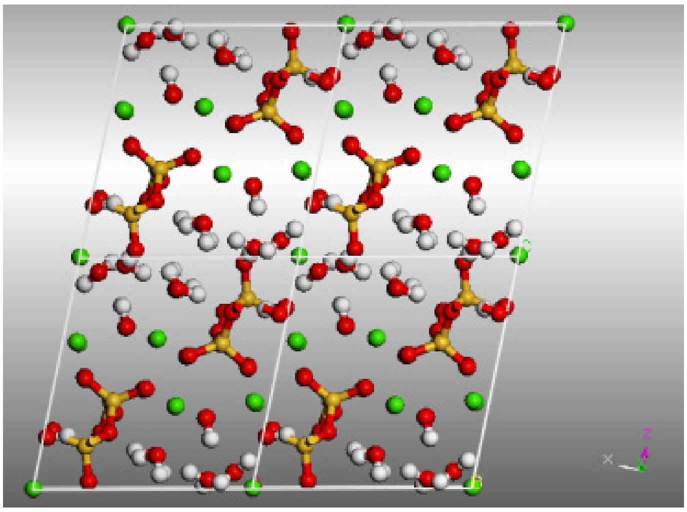

Figure 2.8. Crystal structure of jennite showing calcium (green), silicon (yellow), oxygen (red), and hydrogen (white) [13].

The C-S-H formed during the first hours of hydration, shows a characteristic "sea urchin" structure (see Figure 4.3) that will cover most of the surface of the cement particles. An example of the C-S-H morphology after 32 hours is shown in Figure 2.9. The C-S-H needles have grown into each other and merged into a single matrix, except at larger openings and gaps where single needles can still be visible.

The calcium hydroxide has a layered structure with calcium ions in a close-packed hexagonal structure (Figure 2.10). In the holes between the calcium ions there are hydroxide ions. Every second hydroxide ion is on the top side of the layer with the hydrogen pointing upwards; the other hydroxide ions are on the down side with the hydrogen pointing downwards. The calcium hydroxide forms hexagonal plates during cement hydration.

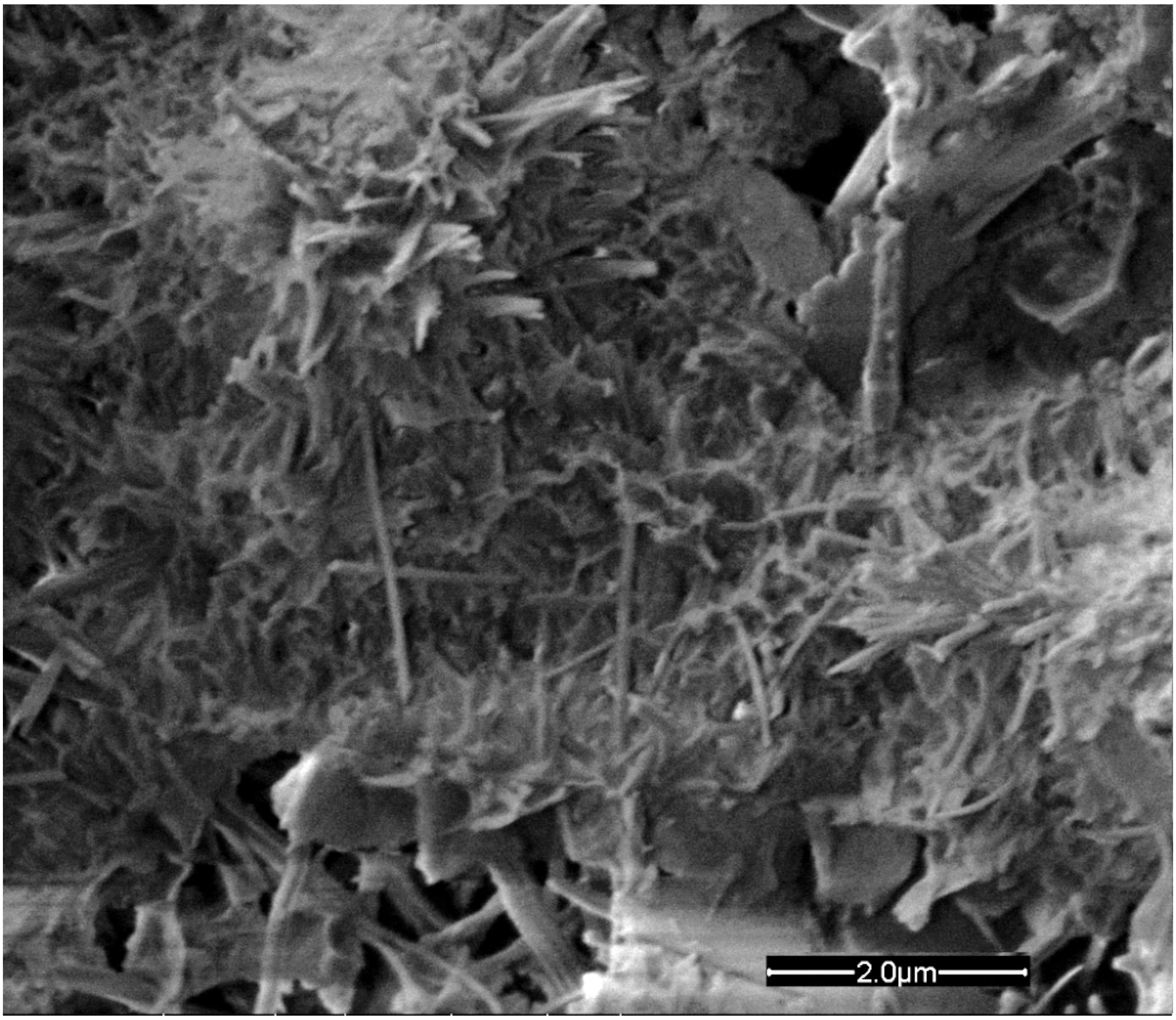

Figure 2.9. SEM images showing C-S-H formation in Portland limestone cement after 32 hours of hydration (from this work).

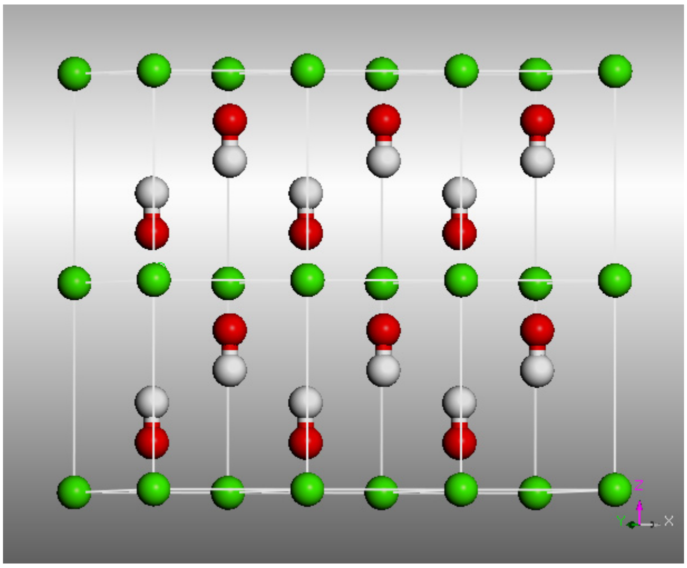

Figure 2.10. Crystal structure of calcium hydroxide showing calcium (green), oxygen (red), and hydrogen (white).

2.3.5 Aluminate

Aluminate ($Ca_3Al_2O_6$, C_3A in cement notation) has a cubic structure containing calcium ions and six-membered alumina rings with the formula $Al_6O_{18}^{18-}$ as shown in Figure 2.11.Aluminate in cement is twofold. It is beneficial in the cement manufacturing, where it forms a liquid during clinkering and thus facilitates the formation of belite and alite in the cement kiln. However, the presence of aluminate in the final product is undesired, since it may react rapidly with water and cause unwanted rapid setting. This can be suppressed by adding a sulfate containing set-controlling agent (usually gypsum) to the cement. Otherwise, the products formed during the hydration of aluminate will interfere with the desired products and decrease the final strength of cement.

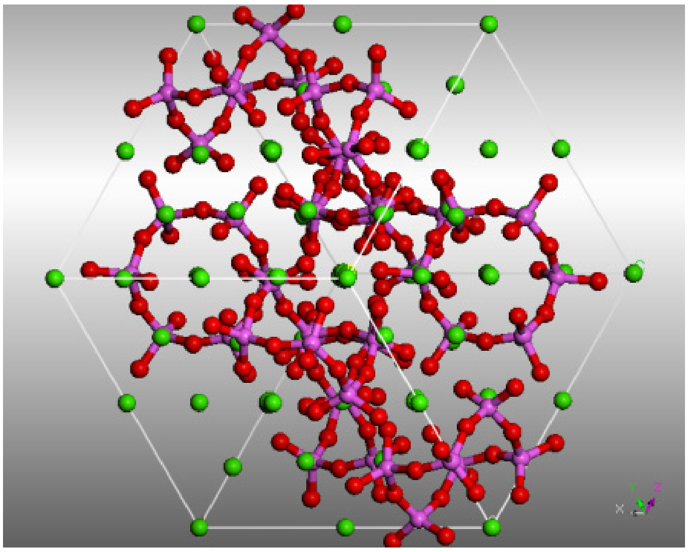

Figure 2.11. Crystal structure of aluminate showing calcium (green), aluminum (purple) and oxygen (red) [14].

2.3.6 Ferrite

Ferrite ($(Al_x, Fe_{1-x})_2Ca_2O_5$, C_4AF in cement notation) is the mineral phase that gives cement its grey colour. The hydration reaction rate of ferrite appears to vary, which could be due to differences in composition or other characteristics [2]. Ferrite forms products similar to those of aluminate, but the reaction rate decreases with increasing F/A ratio. In general the initial reaction rate is fast, but as the hardening process progresses the reaction rate is intermediate between that of alite and belite.

Calcium sulfate

Calcium sulfate plays an important role in the hydration of the aluminate and ferrite minerals. It is added to the cement during grinding, and the heat evolved can cause some of the crystal water to evaporate. Thus, the final cement product may also contain calcium sulfate hemihydrate ($CaSO_4 \cdot 0.5H_2O$) and, in some cases, anhydrite ($CaSO_4$). Anhydrite has two forms, γ-anhydrite and β-anhydrite. Due to similar crystal structure of gypsum (Figure 2.12), hemihydrate and γ-anhydrite, with channels where water can be added or removed, they can easily be transformed into each other. The β-anhydrite has a different structure and cannot incorporate water (Figure 2.13).

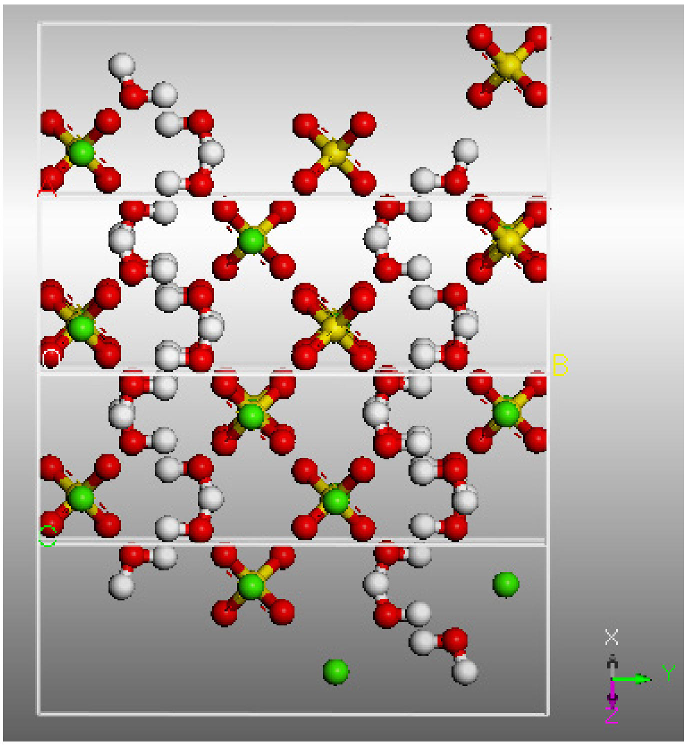

Figure 2.12. Crystal structure of gypsum showing calcium (green), sulphur (yellow), oxygen (red) and hydrogen (white) [15].

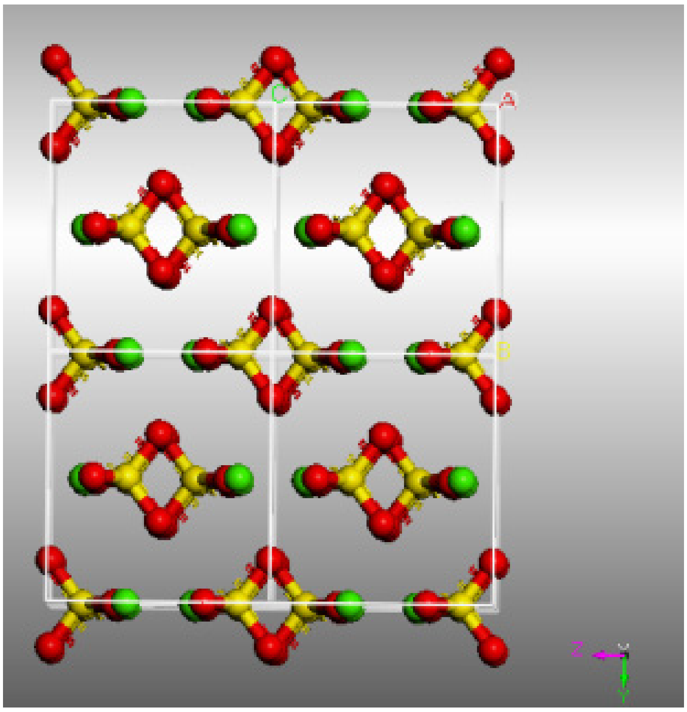

Figure 2.13. Crystal structure of β-anhydrite showing calcium (green), sulphur (yellow) and oxygen (red) [16].

2.3.7 Reaction products of aluminate and ferrite

The hydration of the aluminate and ferrite minerals is more complex than that of the calcium silicate minerals. In this section, some of the reaction products are described.

Formation of AFm phases

AFm (Al_2O_3- Fe_2O_3-mono) phases have the general formula $C_3(A,F)\cdot CaX\cdot xH$ (or $Ca_4(Al,Fe)_2(OH)_{12}\cdot X\cdot yH_2O$), where X denotes one formula unit of a doubly charged anion, or two formula units of a single charged anion. The term "mono" refers to the single formula unit of CaX, where X can be various anions, of which OH^-, SO_4^{2-} and CO_3^{2-} are the most important in cement hydration. The AFm phase consists of similar layers as those in calcium hydroxide, but every third Ca^{2+} ion is substituted with an Al^{3+} ion in an ordered way [2]. The substitution distorts the layer slightly and makes it positively charged. Water and negative ions are position between the layers and balance the positive charge of the calcium-aluminium hydroxide layer. The hydration products formed when pure C_3A is mixed with water are mainly the AFm phases C_2AH_8 and C_4AH_{19} which are converted into C_3AH_6 [2]. In analogous, the hydration of ferrite, C_4AF, forms similar reaction products to those of aluminate, but the reaction rate decreases as the F/A ratio increases.

The presence of some specific ions (e.g. sulfate) in the solution will affect the feasible reactions that take place. During the hydration of cement, the aluminate and ferrite will form AFm containing sulfate ions in the water layer.

Formation of AFt phases

In many types of cement the aluminate and ferrite phases can cause a flash set. This is a rapid set, with strong evolution of heat, and the subsequent development of strength is poor. Since the flash set is associated with the formation of AFm phase plates throughout the paste, it is desired to prevent the formation of the AFm phase. This can be done by letting aluminate and ferrite form the AFt phases (Al_2O_3- Fe_2O_3-tri) with the general formula $C_3(A,F)\cdot 3CaX\cdot xH_2O$. The AFt phases are formed under similar conditions to that of the AFm phases, but at higher ratios of CaX to $C_3(A,F)$. The range of anions that can occupy the X sites is narrower, and singly charged anions can only be accommodated to limited extent.

As the aluminate reacts with gypsum ($C\bar{S}H_2$ ($CaSO_4\cdot 2H_2O$), added to the cement, it will form the AFt phase ettringite, $C_6A\bar{S}_3H_{32}$. The formation of ettringite is presented in reaction (2.3)

$$C_3A + 3\,C\bar{S}H_2 + 26\,H_2O \rightarrow C_6A\bar{S}_3H_{32} \tag{2.3}$$

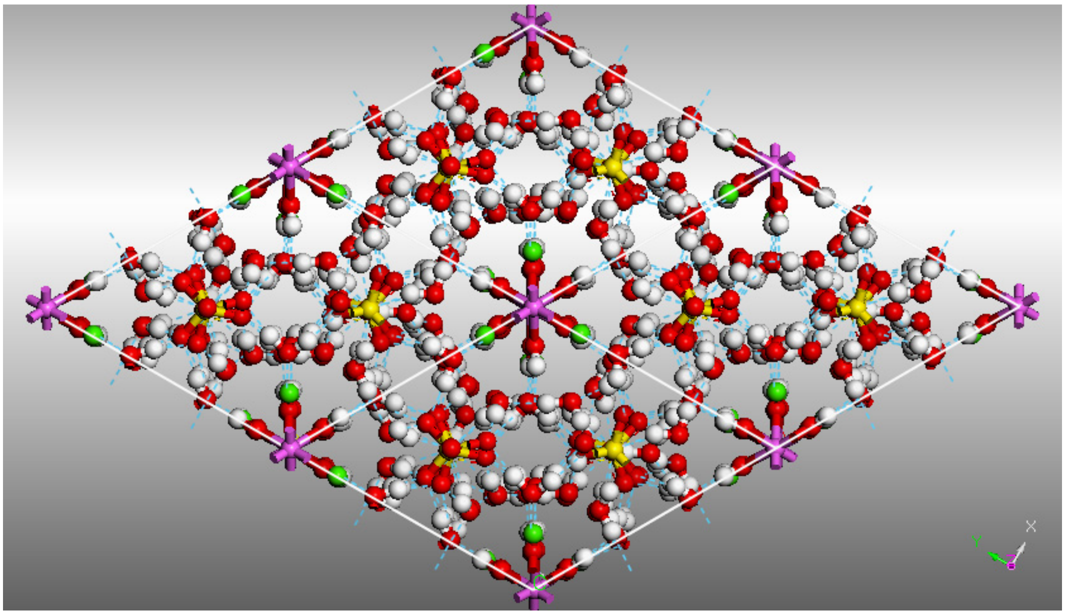

Figure 2.14. Crystal structure of ettringite showing calcium (green), aluminum (purple), sulphur (yellow), oxygen (red) and hydrogen (white) [18].

Subsequently, when all gypsum has reacted, the C_3A reacts with ettringite and CH to form $C_4A\bar{S}H_{12}$ and C_4AH_{13}. The C_4AH_{13} phase may appear either in solid solution with monosulfate or in separate crystals.

$$2\ C_3A + C_6A\bar{S}_3H_{32} + 4\ H_2O \rightarrow 3\ C_4A\bar{S}H_{12} \qquad (2.4)$$

$$C_3A + CH + 12\ H_2O \rightarrow C_4AH_{13} \qquad (2.5)$$

The structure of ettringite (see Figure 2.14) is completely different from that of the monosulfate structure. Ettringite has channels with $Al(OH)_6^{3-}$ and calcium ions. For every aluminium hydroxide ion there are three Ca^{2+} ions, giving the channel a net positive charge. To obtain charge balance in the ettringite structure, there are channels with water and sulfate ions, giving them a net negative charge. All channels are surrounded by water and are ordered in a hexagonal pattern. An ettringite cluster is seen in the SEM image in Figure 2.15.

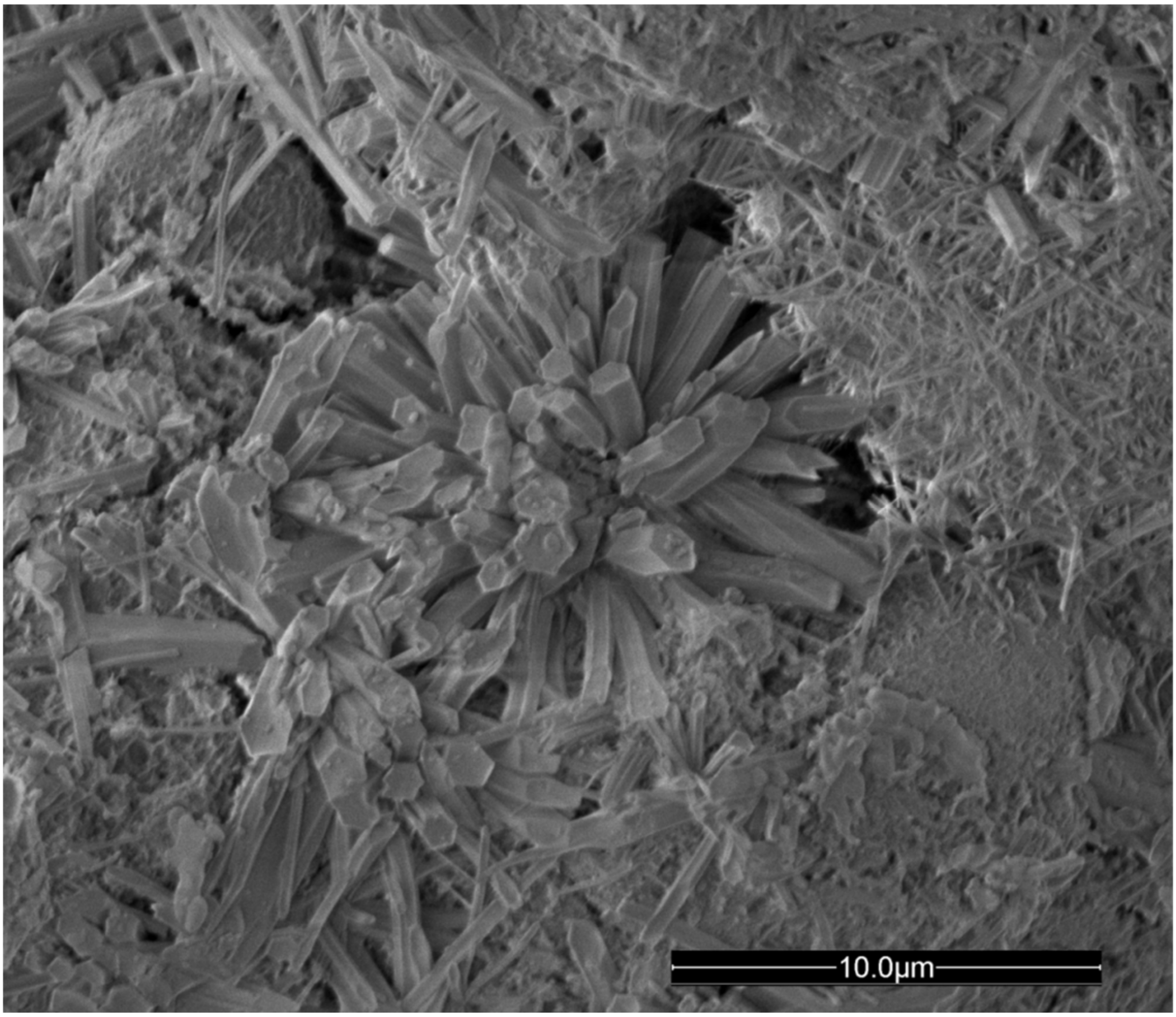

Figure 2.15. SEM image of Portland limestone cement, with an aluminium sulfate accelerator added, hydrated for 8 hours (unpublished work).

2.4 **Calcium Carbonate**

The carbonation of Portland cement is a naturally occurring process during the aging of a concrete structure. It changes the physical and chemical properties of the cement. During the carbonation process $CaCO_3$ is formed and other carbonate phases are expected to be negligible. The carbonation may also induce corrosion of steel reinforcing bars, due to the reduction of alkalinity, which may cause severe damage to a structure.

Calcium carbonate ($CaCO_3$) has three crystalline anhydrous forms [18–20]: calcite (Figure 2.16), aragonite (Figure 2.17) and vaterite (Figure 2.18). Of these calcite is the stable form at normal atmospheric conditions. It is an abundant mineral and is a raw material to Portland cement. It can also be mixed with the already produced cement as filler. The cement is then called Portland limestone cement, and it is that type that has been used throughout this work.

There are also two water containing forms of calcium carbonate: monohydrocalcite and ikaite [21–23]. Both are meta-stable towards the anhydrous forms at normal atmospheric conditions. The sixth form of calcium carbonate is amorphous.

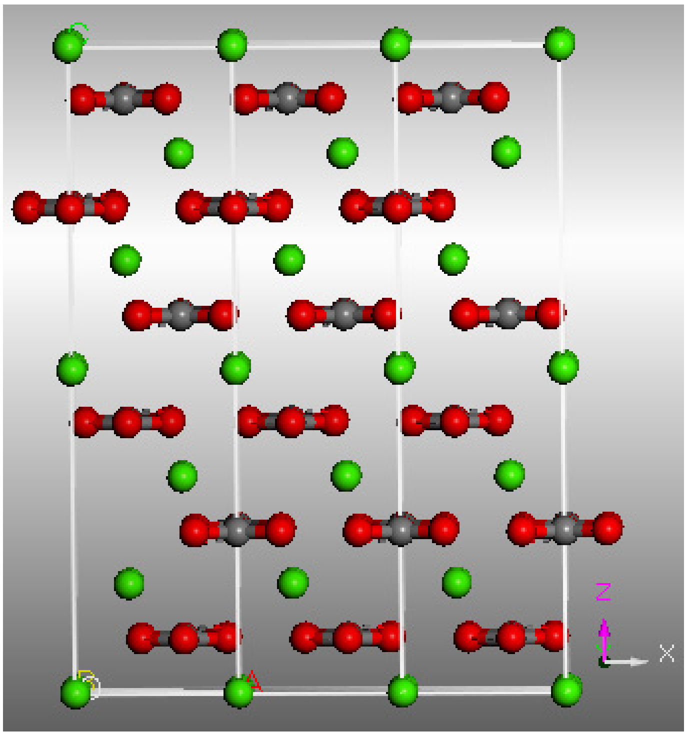

Figure 2.16. Crystal structure of calcite showing calcium (green), carbon (grey) and oxygen (red) [24].

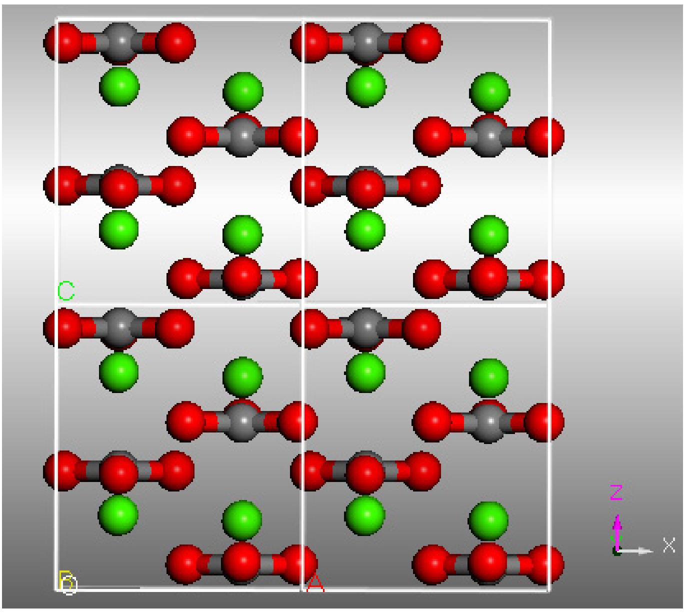

Figure 2.17. Crystal structure of aragonite showing calcium (green), carbon (grey) and oxygen (red) [25].

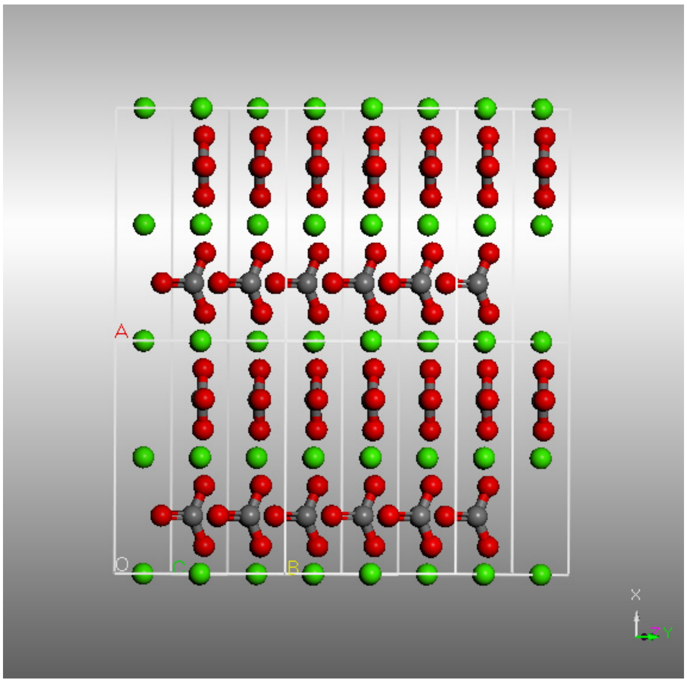

Figure 2.18. Crystal structure of vaterite showing calcium (green), carbon (grey) and oxygen (red) [26].

2.5 Colloidal Nano-Silica in Cement

Colloidal nano-silica (CNS) consists of SiO_2-particles suspended in water. The size of the particles can be controlled during manufacturing and can range from a few nanometres to several hundred nanometres. Addition of CNS has several positive effects on cement and concrete. It accelerates the early hydration of cement [27–29] and increases the compressive and flexural strength of concrete [30–36]. Most cement manufactures are trying to dilute their cement with other reactive waste products, such as ash or slag, to meet the demands of more environmentally friendly and sustainable cement. However, the waste products often contain alkalis. The reaction of alkalis with silica in the aggregates can cause expansive phases that damage the concrete (alkali-silica reaction, ASR). There are therefore limits on the amount of alkalis that are allowed in the cement in most cement standards and this limits the amount of cement that can be replaced by waste products. CNS has been shown to counteract the ASR [31].

Corrosion of reinforcement bars is a very common reason for concrete damages. The corrosion is greatly accelerated in the presence of chlorides. The addition of CNS gives a denser concrete with less porosity [32, 36], resulting in decreased chloride ion penetration and water absorption [30, 35].

CNS forms a gel when it is added to solutions containing positive ions. This prevents bleeding and segregation of the concrete mortar [37]. However, it also affects the rheology of the mortar, making it thicker and less fluid. To obtain a desired consistency more water or plasticisers must therefore be added.

3 Experimental Techniques

3.1 Material and Sample Preparation

The Portland cement used in this work was a Portland limestone cement, “byggcement Std PK Skövde CEM II/A-LL 42,4 R´´, from Cementa AB.

The cement samples were mixed with distilled ionized water in an automatic/manual mortar mixer 39-0031 from ELE International, at 140 rpm on the mixing blade and 62 rpm on the mixing head. The w/c (water to dry cement by weight) ratio was 0.4 (Papers I–III, V) or 0.5 (Paper IV). In some studies the cement paste was blended with a hand-mixer and/or by hand. Casting was normally made in plastic dishes, 35 mm in diameter. The thickness of the paste in the dishes was approximately 2–3 mm. Lids were placed over the dishes while they were hydrated to prevent water from evaporating

The colloid nanosilica particles were supplied by AkzoNobel Pulp and Performance Chemicals AB (former Eka Chemicals AB). The used products are called “Cembinder 50” (narrow particle distribution (size 5 nm), dry content 15%) and “Cembinder 8” (broad particle distribution (size 10-100 nm), dry content 50%).

The freeze-drying of the hydrated cement samples was performed by immersion the samples into liquid nitrogen, followed by vacuum drying. The freeze-drier was constructed by connecting a vacuum pump to a vacuum chamber. The samples were normally freeze-dried overnight and measurements were conducted the following day.

3.2 Fourier Transform Infrared (FTIR) Spectroscopy

3.2.1 Motivation

Cement contains several chemical components that contain various functional groups, such as Si-O, SO_4, H_2O, OH, Al-O and CO_3, which are infrared active. The absorbed infrared wavelengths of the functional groups are dependent on the chemical surroundings of the group. Hence, there will be shifts of the absorption bands of the functional groups e.g. the crystalline clinker phases is altered to the water containing, amorphous hydration phases. Infrared spectroscopy is therefore a suitable tool to provide information about the hydration of cement. The Fourier transform infrared (FTIR) technique is also a quantitative/semi-quantitative method, which makes it possible to estimate the amounts or relative amounts of the constituents in the samples. In this case the Lambert-Beer law; $A = \varepsilon \cdot c \cdot l$, can be applied, where A: absorbance, ε: absorptivity coefficient, c: concentration and l: path length. In this work the FTIR has been used as a semi-quantitative method to study the cement hydration processes.

3.2.2 Basics

A chemical bond may be regarded as an oscillating spring that can vary in distance and has an equilibrium distance where the bond is relaxed. Thus the atoms in the molecules may be considered as balls, connected by springs that vibrate with frequencies that are dependent on the bond strength and the masses of the atoms. More specific it is the *reduced mass* defined by $m_{reduced}=m_{atom1}m_{atom2}/(m_{atom1}+m_{atom2})$ that influences the vibration frequency. The stronger the bond between the atoms and the smaller the reduced mass, the higher the value of the vibration frequency. If $m_{atom1} << m_{atom2}$, the reduced mass will be approximately equal to m_{atom1}. This is almost always the case when hydrogen atoms are bonded to other elements.

Quantum mechanics states that vibrations only occur at some specific frequencies. The energies for these possible vibrations are given by equation (3.1).

$$E_{vib} = \frac{h}{2\pi}\sqrt{\frac{K}{m_{reduced}}}\times\left(n+\frac{1}{2}\right) \tag{3.1}$$

h is Planck's constant, *K* is the bond strength between the atoms and *n* is an integer.

If there is a polarization over the bond, meaning that there is a small positive charge on one of the atoms and a correspondingly small negative charge on the other atom, the atoms can absorb electromagnetic radiation and go from one energy level to another. The energy ΔE needed for a transition from an energy level with $n_{initial}$ to an energy level with n_{final} is given by equation (3.2).

$$\Delta E = \frac{h}{2\pi}\sqrt{\frac{K}{m_{reduced}}}\times\left(n_{final}-n_{initial}\right) \tag{3.2}$$

Transitions between energy levels only occur if the energy of the electromagnetic radiation matches this energy difference exactly. The energy of electromagnetic radiation is given by equation (3.3), where *f* is the frequency of radiation.

$$\Delta E = hf \tag{3.3}$$

The connection between frequency and wave number *k* is presented in equation (4) where *c* is the speed of light.

$$f = ck \tag{3.4}$$

At room temperature almost all molecules are in their ground vibration state ($n_{initial}=0$). The majority of all transitions in molecules are between the ground state and the first excited state ($n_{final}=1$). Combining this with equations (3.2)–(3.4) the wave number of the light that can excite the vibration is given by equation (3.5).

$$k = \frac{h}{2\pi c}\sqrt{\frac{K}{m_{reduced}}} \qquad (3.5)$$

This wave number typically lies in the infrared region of the electromagnetic spectrum.

When more than two atoms are involved in the vibration, the molecules vibrate in all three dimensions. For non-linear molecules there are therefore 3N-6 independent vibration modes, where N is the number of atoms in the molecule. The same applies to groups of bonded atoms within a molecule. If the molecule or group is linear there are 3N-5 vibration modes. The vibration normal modes are often denoted υ_1, υ_2, υ_3, etc. The vibration modes of water are shown in Figure 3.1.

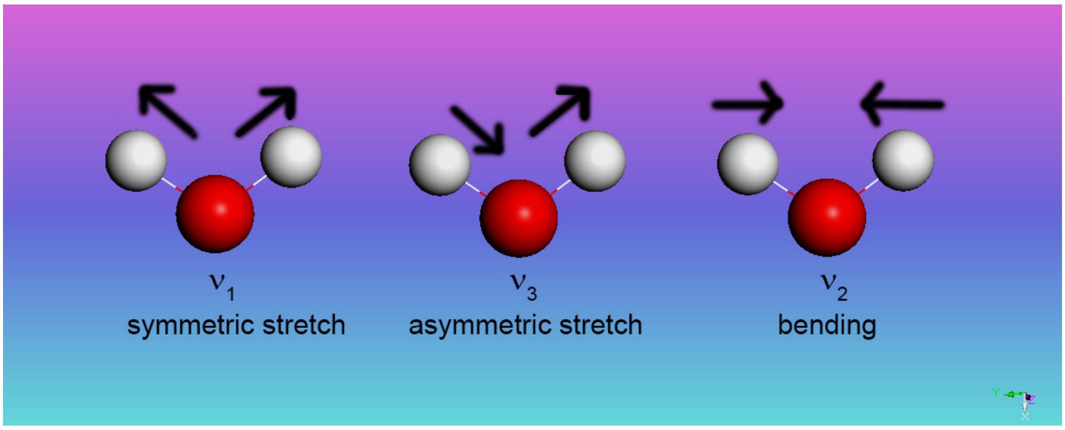

Figure 3.1. Vibration modes of water.

A molecule absorbs electromagnetic radiation with characteristic frequencies. This can be used to identify molecules or specific groups present in a compound or sample. Sending electromagnetic radiation of known frequency through the sample and measuring the change in intensity of the radiation provides the characteristic wave numbers of an infrared (IR) spectrum. The IR spectra are usually presented as plots of intensity versus wave number. Two substances absorbing at the same wave numbers are most likely identical. The IR spectrum of a compound is therefore called its fingerprint.

3.2.3 Measuring technique

The radiation source in an interferometer (FTIR-spectrometer) is a vital part of the instrument and it usually consists of a ceramic element. The element is heated to several hundred degrees centigrade. Due to the high temperature it starts to emit electromagnetic radiation in the infrared region. The light from the radiation source hits a beam splitter that reflects about half of the light while the rest of the light passes straight through the splitter. One part of the beam proceeds to a fixed mirror and the other part to a mirror that can be moved forward and backward, generating a path difference, see Figure 3.2. The mirrors reflect the light back to the beam splitter where they will recombine to form an interference pattern. This pattern will be determined by the path difference of the two beams. Then the combined beam traverses the sample, where the sample will absorb light of different frequencies depending on what molecules the sample contain, and then proceed to the detector that registers the signal. To determine the absorbed frequencies of the sample, a background spectrum with no sample has to be collected, either before measurement or parallel with the measurement.

For a single frequency the interference pattern is a sine wave with a maximum when the two beams are in phase and a minimum when they are out of phase by 180 degrees. The beams are in phase when the path difference is equal to the wavelength multiplied by an integral.

For a broad band source like the ceramic element the interference pattern is the sum of the sine waves for all the frequencies present. This interferogram consists of a strong signal where the path difference is zero, falling rapidly on either side. To obtain an IR spectrum the interferogram is transformed with a Fourier transform, hence the name of the method. The interferogram is measured by recording the detector signal as a function of the path difference between the two beams. The signal has to be sampled at precise intervals corresponding to equal steps in path difference. For signal averaging successive interferograms have to be measured at exactly the same points. This is achieved by using a helium-neon laser as a reference. Monochromatic radiation from the laser, with a wavelength of 632.8 nm, travels the same optical path as the infrared beam. A separate detector measures the interferogram produced by the laser, giving a sinusoidal signal with maxima separated by the laser wavelength. This signal is used to trigger the sampling of the infrared signal very reproducibly.

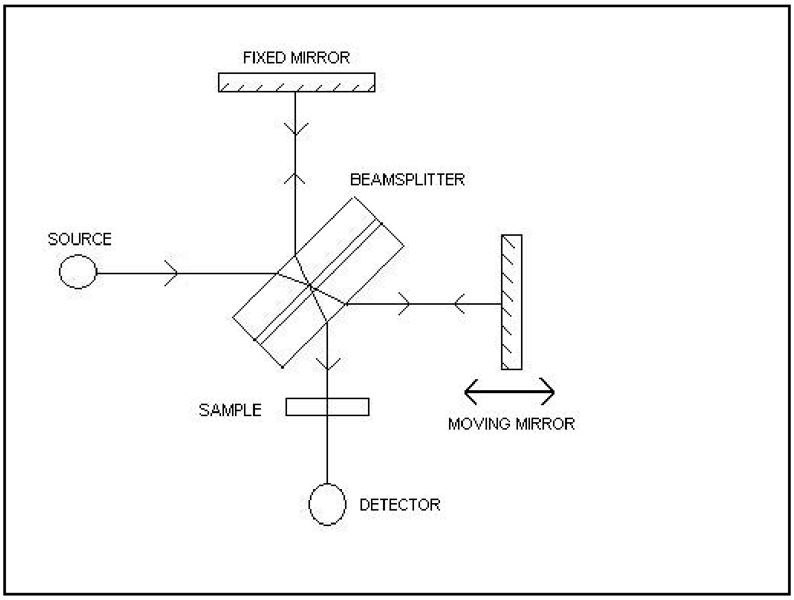

Figure 3.2. Schematic picture of an FTIR-spectrometer.

3.2.4 DR-FTIR

The diffuse reflection FTIR (DR-FTIR) is used to analyse powdered samples. The powdered sample is directly put into a sample holder, which is placed into an insert for DR-FTIR in the spectrometer, Figure 3.3. The beam is focused on the sample by a concave mirror. The sample will then absorb some of the infrared light and reflect the rest. The reflected light is again focused by a concave mirror and proceeds to the detector where the signal is registered.

A difference spectrum, where a spectrum is subtracted from another spectrum, greatly enhances the differences of two spectra and is used extensively in this work. To produce an appropriate difference spectrum the sample preparation must be performed in a reproducible manner. It was found that the best reproducibility was achieved when the sample was very finely ground, but not so fine that it started to cake. The procedure is to slightly overfill the sample cup, followed by gently tapping it against the table to fill it entirely. To produce a flat surface the excess is scraped off. The sample cup is again tapped gently against the table and the sample is then ready for measurement. The sample should not be pressed, as this will affect the porosity of the sample and it is also difficult to press in a reproducible manner. The effect of pressure can be seen at the lower wavenumbers (<1000 cm^{-1}).

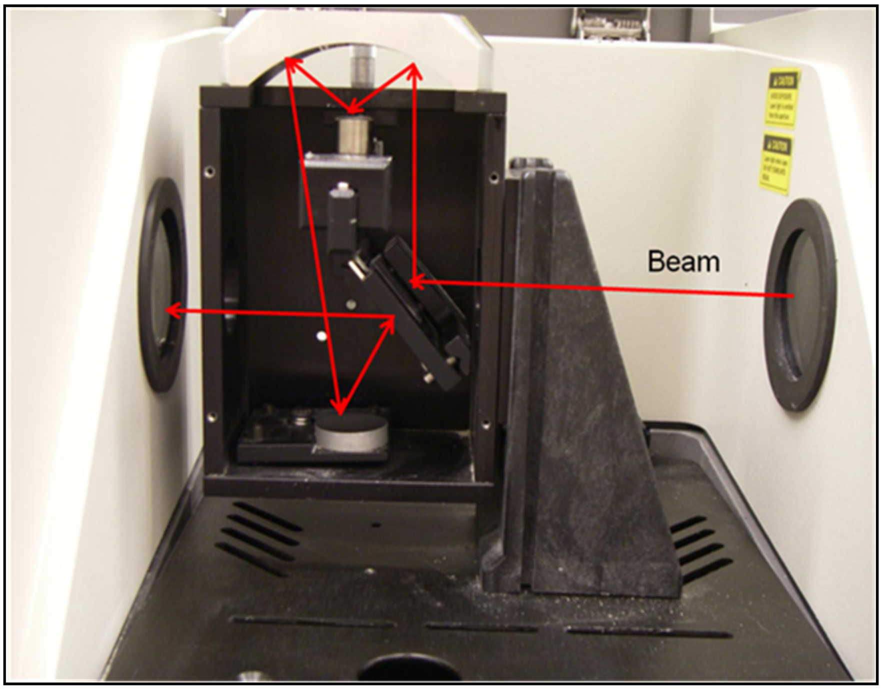

Figure 3.3. Picture of an insert for diffuse reflectance FTIR, where the path of the beam is indicated (red).

3.2.5 ATR

In attenuated total reflection (ATR) FTIR spectroscopy the sample is placed on a crystal, the so-called internal reflection element (IRE). Various materials can be used as IRE, such as silicon, germanium and zinc selenide. To obtain total internal reflection the IRE must have larger refractive index than the sample. Commonly, the IRE material is chosen to have large chemical and mechanical resistance. In this work diamond was used as IRE, since it has a high refractive index of (2.41) [38] and excellent chemical and mechanical resistance. This makes it suitable for measurements on the hard and alkaline cement samples.

The infrared radiation only passes through the IRE and not through the sample. The radiation interacts with the sample through an exponentially decaying electrical field extending from the surface. This field is referred to as the evanescent wave. The penetration depth of the evanescent wave is directly proportional to the wavelength. Therefore absorption at lower wave numbers (i.e. longer wavelengths) is larger, and absorption at higher wave numbers is suppressed. To obtain relative peak intensities that are similar to those obtained by transmission FTIR (described below), the ATR spectrum is multiplied by the wave number. This correction is usually included in the spectrometer control software.

To obtain a high quality ATR spectrum the contact between the IRE and the sample is vital, as the evanescent wave decays rapidly from the IRE surface. This is not a problem for liquid samples, but for solid samples the clamping can be problematic, especially for hard samples such as cement. Even if the cement is ground to a fine powder there can be difficulties in obtaining good reproducibility, as the porosity can vary with applied pressure. The amount of sample in contact with the IRE surface will then also vary. However, if the powder is ground fine enough, the reproducibility will be sufficient to produce difference ATR spectra.

3.2.6 Transmission FTIR

The transmission FTIR can be used to measure infrared active gases, liquids and solids. A solid infrared active material can be measured by blending a small amount of the powder with an infrared transparent soft salt (e.g. KBr and KCl). The mixture is then pressed into a solid disc, and can be measured by transmission FTIR. However, to obtain good quantitative reproducibility the sample must be evenly distributed in the salt and the disc should be evenly compacted and pressed. The sample can be altered by this procedure, as ions from the salt can substitute into the sample during pressing. The transmission FTIR technique can therefore be considered to be a more precarious method compared to DR-FTIR and ATR.

3.3 Vicat

Vicat is a fast and down-to-earth method to determine the setting of cement. The mortar or cement paste are prepared and put into a mould (see Figure 3.4). A needle of standardized shape is pressed into the mortar with a standardized force during regular time intervals. The penetration depth of the needle is recorded and plotted against time. When the needle no longer is able to penetrate into the mortar the cement is considered to be set. The Vicat apparatus used in this work was a Vicatronic automatic recording apparatus E040. The measurements were performed in a 40 mm mould with a calibrated weight of 300 g and a cylindrical needle with a flat tip of area 1 mm^2. A typical sample size is 300 g of cement.

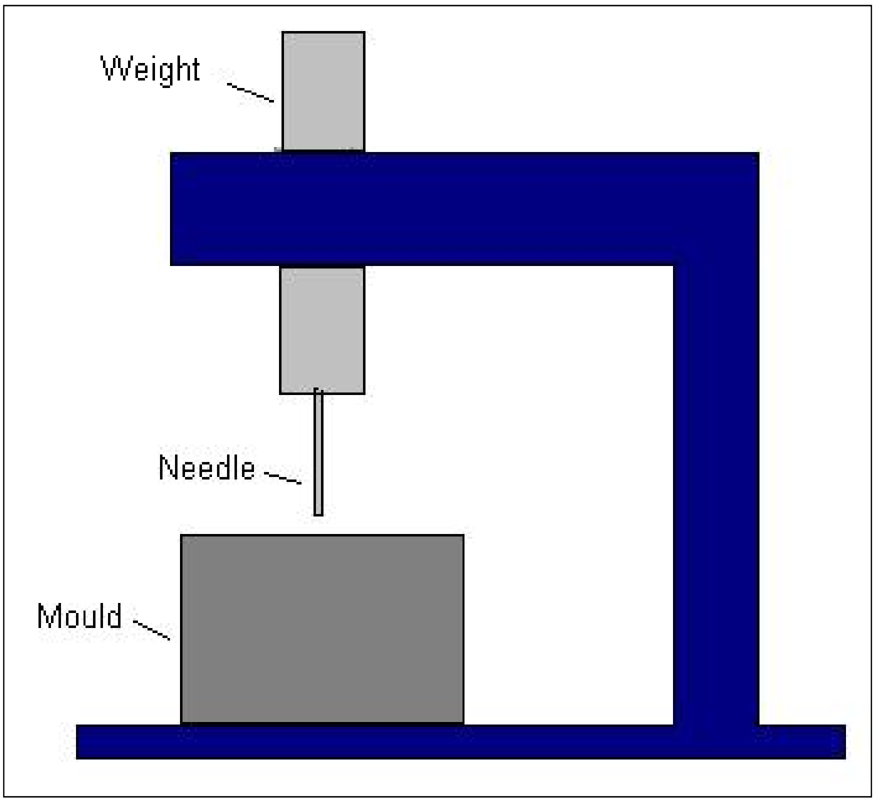

Figure 3.4. Schematic picture of a Vicat apparatus.

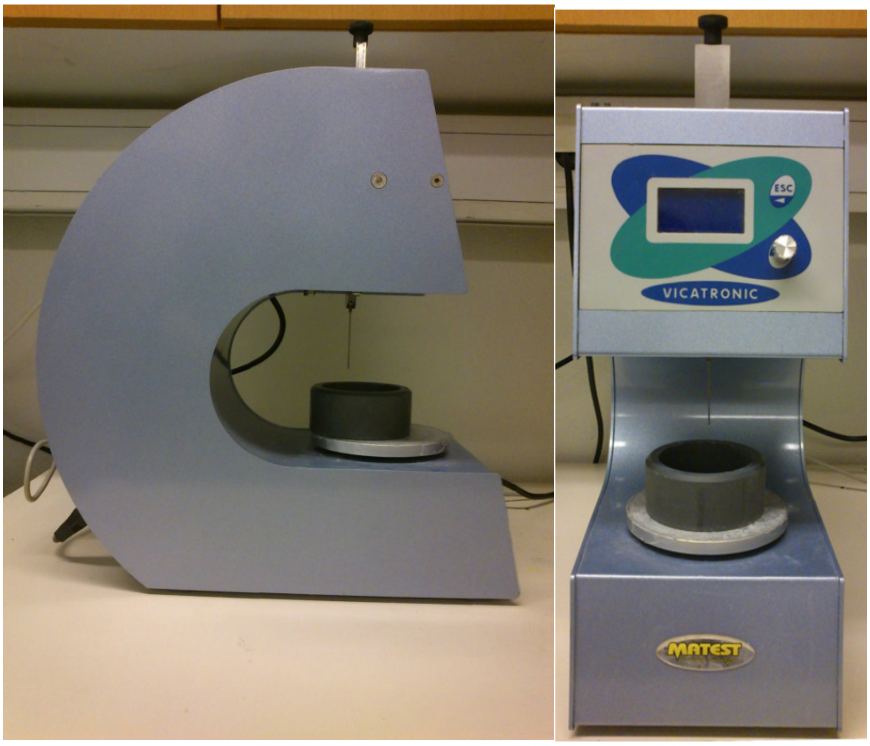

Figure 3.5. Vicat apparatus used in the present work.

3.4 **Isothermal Calorimetry**

Chemical and physical processes generally include heat exchange with the surrounding. In cement the evolution or absorption of heat is correlated to distinct chemical and physical processes such as hydration, carbonation or phase transitions. The flow of heat is therefore an important parameter to consider in understanding the complex nature of cement.

To measure the flow of heat in a cement sample a special designed calorimeter has been used in this work. The calorimeter consists of a sample holder, a heat-flow sensor and a heat sink. The sample holder is in thermal contact with the heat-flow sensor which in turn is mounted on the heat sink, and all are placed in an isolated container (see Figure 3.6). The temperature in the container is kept constant by a thermostat whose temperature was controlled by a thermoelectric air-air heater/cooler (AA-100-24-22, SuperCool AB, Göteborg , Sweden). This means that all processes that involve loss or gain of heat are studied at a fix temperature. Hence, this method is called “isothermal calorimetry”.

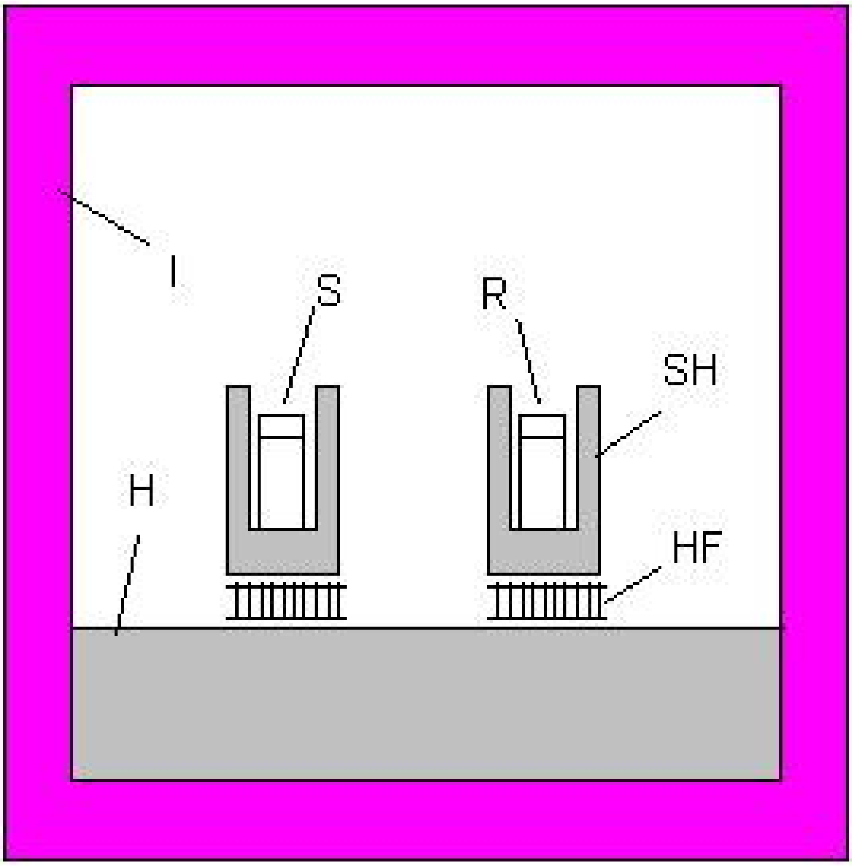

Figure 3.6. Schematic image of an isothermal calorimeter with a heat-sink (H), heat-flow sensor (HF), sample holder (SH), sample (S), reference (R) and isolated container (I).

Temperature fluctuations in the calorimeter will affect the measurements and may cause severe noise in the output signal. To reduce the noise level in the thermograms a reference sample is normally used. The reference sample should not evolve any heat and have a heat capacity similar to the examined sample. In this work a defined amount of water was used as a reference sample. By using this experimental set-up all temperature fluctuations will affect the sample and the reference sample in a similar manner. The final thermogram is obtained by subtracting the signal of the reference from the signal of the sample.

The calorimeter was arranged so that several samples in 20 cm^3 ampoules could be measured and removed without opening the isolated container. A more detailed description of isothermal calorimetry measurements has previously been described [39].

3.5 Scanning Electron Microscopy - SEM

The scanning electron microscope (SEM) is a powerful tool for imaging and chemical analysis in cement research. With a high resolution (down to 1nm) and a large depth of focus, it enables a detailed study of the rough surfaces of e.g. the formed calcium silicate hydrate (C-S-H). This is difficult to study using an optical microscope.

The SEM is a microscope that uses electrons instead of light to form an image and it is used under vacuum conditions. A beam of electrons is generated by placing a high electric potential difference between a tip and a plate with an aperture. The potential can range from a few hundred volts to several tens of kilovolts. The electron beam travels through the microscope, where a series of magnetic lenses and apertures focus the electron beam. As the electron beam hits the sample, it will scan the surface in a raster scan pattern, hence the name of the technique.

When the focused electron beam hits the sample, the beam electrons will interact with the atoms at or near the surface of the sample and a variety of signals is generated. There are mainly three signals measured in the SEM: secondary (SE) and backscattered (BSE) electrons (for imaging) and characteristic X-rays (for chemical analysis). They originate from different depths and volumes in the sample and provide different information about the sample. The SEM images in this work are all taken in secondary electron detection mode.

Using secondary electrons for imaging will show morphology and surface topography of a sample. The secondary electrons originate from the outermost part of the surface and are generated when the beam electrons lose energy by inelastic collisions in the sample and knocks out secondary electrons from the atoms. It is primarily the incident beam electrons that knock out the secondary electrons, although backscattered electrons can also contribute. The energy of secondary electrons is typically 50 eV or less. It is only the secondary electrons generated close to the sample surface that will have sufficient energy to leave the sample. The emitted secondary electrons are attracted to the detector by a positive electric potential and induce a signal. This results in a topological view of the surface that resembles a normal photography. In this work a SEM instrument, FEI Quanta 200 FEG ESEM, is used to investigate the surface morphology of cement. In combination with other analytical techniques this provides an understanding of the hydration process of cement.

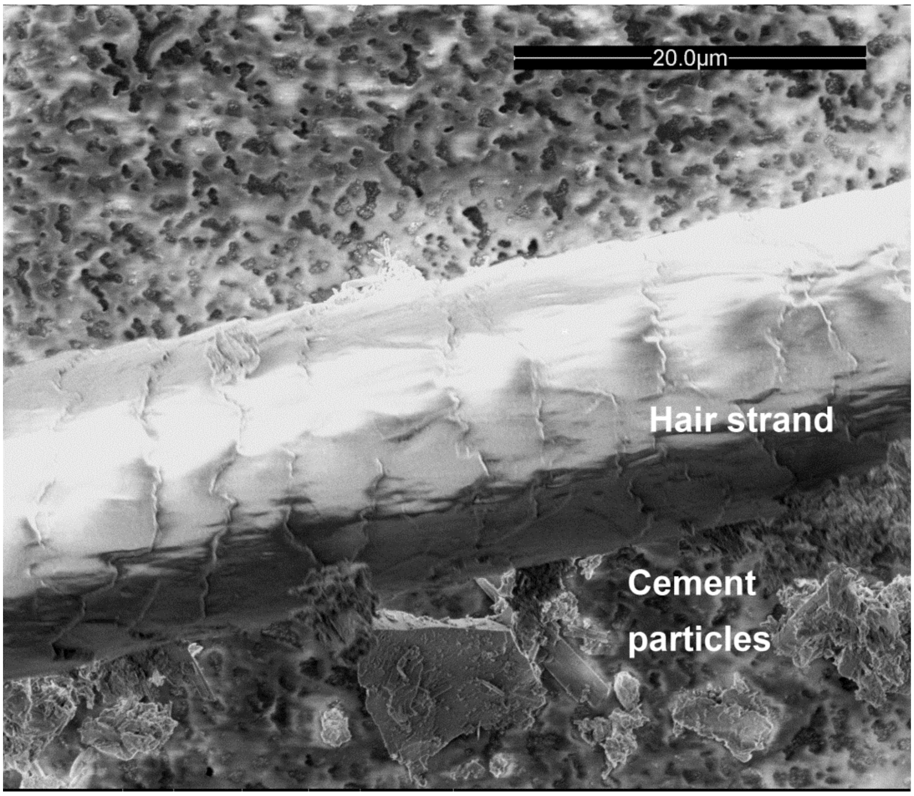

Figure 3.7. An SE image showing cement particles and a human hair strand (labelled). The upper part of the image shows the carbon tape.

The sample surface will be charged by the electron beam as electrons are either knocked out or absorbed. This will especially affect the low energy secondary electrons. This will produce bright spots and can also distort the image. To remove charge build-up the sample stub is connected to electric earth. However, poorly conducting material such as cement will still suffer of charge build-up because the electrons will only slowly be removed from the sample. The sample should be very small to counter this. In this work the cement was crushed and sprinkled on a conducting carbon tape. Figure 3.7 shows a SEM image of a human hair strand with some cement particles in the lower part of the picture. It illustrates the small size of the cement particles. The upper part of the picture shows the surface of the carbon tape. To decrease the charge build-up further the accelerating voltage of the electron beam used was 2—6 kV, which is rather low.

It is also possible to coat the sample with a conducting nano-layer of conducting carbon or gold to lower charge build-up. However, this can affect the structure of the surface and it was not done in this work.

4 Summary of Papers

The tables below are provided to facilitate interpretation of FTIR spectra of cement and its hydration products. Note that it is not only the position of the peak that is relevant; the shape and correlation to other peaks are also important in the interpretation.

Wavenumber [cm^{-1}]	possible assignment
656-658	υ_4 of SiO_4
714	υ_4 of CO_3
847-848	Al-O, Al-OH
877-878	υ_2 of CO_3
1011-1080	polymerized silica
~1100-1200	υ_3 of SO_4
1200-1202	syngenite, thenardite
1400-1500	CO_3
1620-1624	υ_2 of water in sulphates
1640-1650	υ_2 H_2O
1682-1684	υ_2 of water in sulphates
1795-1796	$CaCO_3$
2513-2514	$CaCO_3$
2875-2879	$CaCO_3$
2983-2984	$CaCO_3$
3319-3327	syngenite, thenardite
3398-3408	υ_3 of H_2O, capillary water
3457	$\upsilon_1+\upsilon_3$ of H_2O
3554	υ_3 of H_2O in gypsum
3611	bassanite
3641-3644	$Ca(OH)_2$

Symbol	Wave number and assignment
I	842-910 cm^{-1}: ν_2 - out of plane vibration of CO_3^{2-}
II	1070-1085 cm^{-1}: ν_1 - symmetric stretching of CO_3^{2-}
III	1200 cm^{-1} narrow peak: unknown, formed directly after addition of water to cement 1200 cm^{-1} broad peak: Si-O stretching of condensed silica
IV	1425-1590 cm^{-1}: ν_3 - asymmetric stretching of CO_3^{2-}
V	1600-1700 cm^{-1}: bending mode of H_2O
VI	1800 cm^{-1}: $\nu_4+\nu_1$ of CO_3^{2-}
VII	2500 cm^{-1}: $\nu_4+\nu_3$ of CO_3^{2-}
VIII	Broad band >3000 cm^{-1}: stretching of OH
IX	3643 cm^{-1}: stretching of OH in $Ca(OH)_2$
X	1100-1200 cm^{-1}: S-O stretching of SO_4^{2-}

Tables (from Table 1 Paper II and Table 1 Paper IV) with possible assignments of FTIR peaks.

4.1 Time Resolved Analysis of Cement Hydration by *ex situ* DR-FTIR

4.1.1 Sampling while hydrating by freeze-drying

As long as a cement paste contains water it continues to hydrate. To stop the hydration at a selected instance the water must be removed or the temperature must be lowered so that the water freezes. Several methods for removing the water have been used. The simplest is to place the sample in a furnace where the temperature is kept above the boiling point of water. However, this greatly affects the structure of the hydration products. A second possibility to stop the hydration is by replacing water with another solvent, such as methanol or acetone. The solvent can then be removed by evaporation. The draw-back of such a technique is the difficulty it represents to remove all of the solvent, which in turn may complicate the subsequent analyses. The latter is particularly true when organic additives are involved.

In the present work, the hydration reactions was stopped by immersing samples of cement paste in liquid nitrogen, with a temperature of -196 ºC. The samples should be small to quickly cool below the freezing point of water. Also, rapid cooling prevents ice-crystals to form, which otherwise could destroy the micro-structure of the sample. To prevent the hydration from starting again when the sample is reheated to room temperature, the water must be removed. This was done by placing the frozen samples in a low-pressure chamber, where the pressure is significantly lower than the pressure of the triple point of water (612 Pa). At this pressure the water can only exist in solid and gaseous form. By continuously pumping, the free water subliming from the solid is removed.

After freeze-drying the samples are in dry solid form and thus further cement hydration cannot takes place. This makes it possible to use several measuring techniques, including SEM and diffuse reflection FTIR, as was done in Paper II. If the sample is stored in a dry environment, preferably free of carbon dioxide, it becomes possible to measure also after longer periods of storage.

4.1.2 Complementary observations by SEM, Vicat and *ex situ* DR-FTIR (Paper I and Paper II)

In Paper I it was shown that good reproducibility is achieved if the sample is sufficiently grinded and a particular routine is employed to fill the sample cup. This was demonstrated by comparing differential spectra acquired at the same hydration time of samples taken from the same batch as well as samples of different batches. This simple yet important property allows for the observation of differential effects resulting from the introduction of additives. Paper II shows that the hydration indeed stops very quickly, as there is possible to see differences between the samples taken after 15 seconds and 30 seconds of hydration (see Figure 4.1)

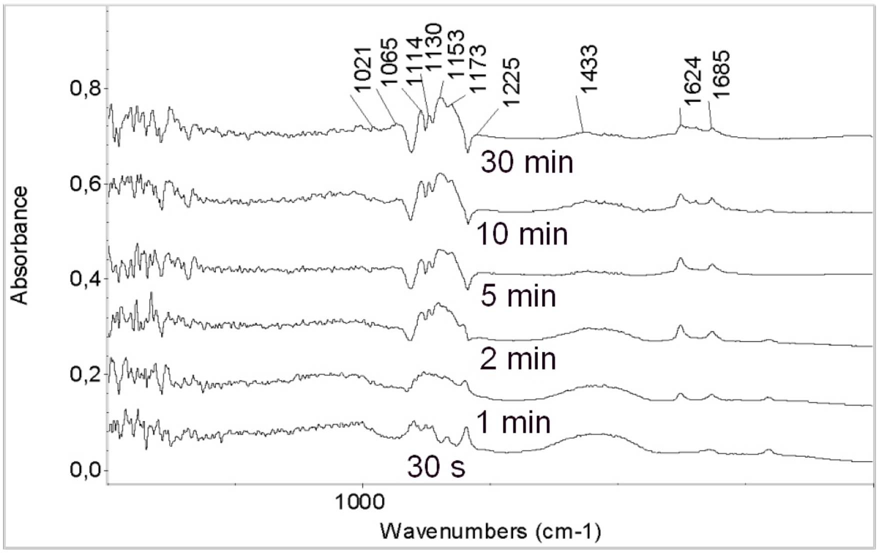

Figure 4.1 (from Figure 5 in Paper II). Difference spectra in the range 500–2000 cm^{-1} where the absorbance spectrum of the freshly mixed cement (15 s) has been subtracted from the absorbance spectra of cement with hydration times from 30 s to 30 min. The spectra are shown offset for clarity.

Paper II also utilizes the possibility to measure with different techniques on the same sample. With DR-FTIR it was found that when the cement paste sets, which was determined using Vicat, there was a shift in the silicate region (900–1000 cm^{-1}) from lower to higher wave number (see emerging "dip-hump" structure in Figure 4.2). The shift was coupled with incorporation of water seen as an increase of the water bending mode centred at 1650 cm^{-1}. This together was taken to indicate that C-S-H had started to form. This was confirmed by using SEM on the same samples, as the characteristic “sea urchin” structure of C-S-H was observed to form at the same time (see Figure 4.3).

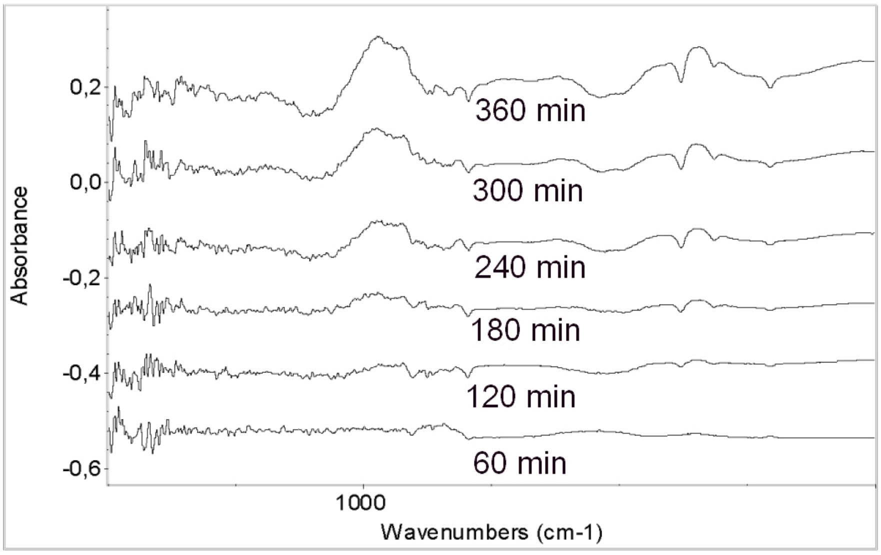

Figure 4.2 (Figure 6 in Paper II). Difference spectra in the range 500–2000 cm^{-1} where the absorbance spectrum of cement hydrated for 30 min has been subtracted from the absorbance spectra of cement with hydration times from 60–360 min. The spectra are shown offset for clarity.

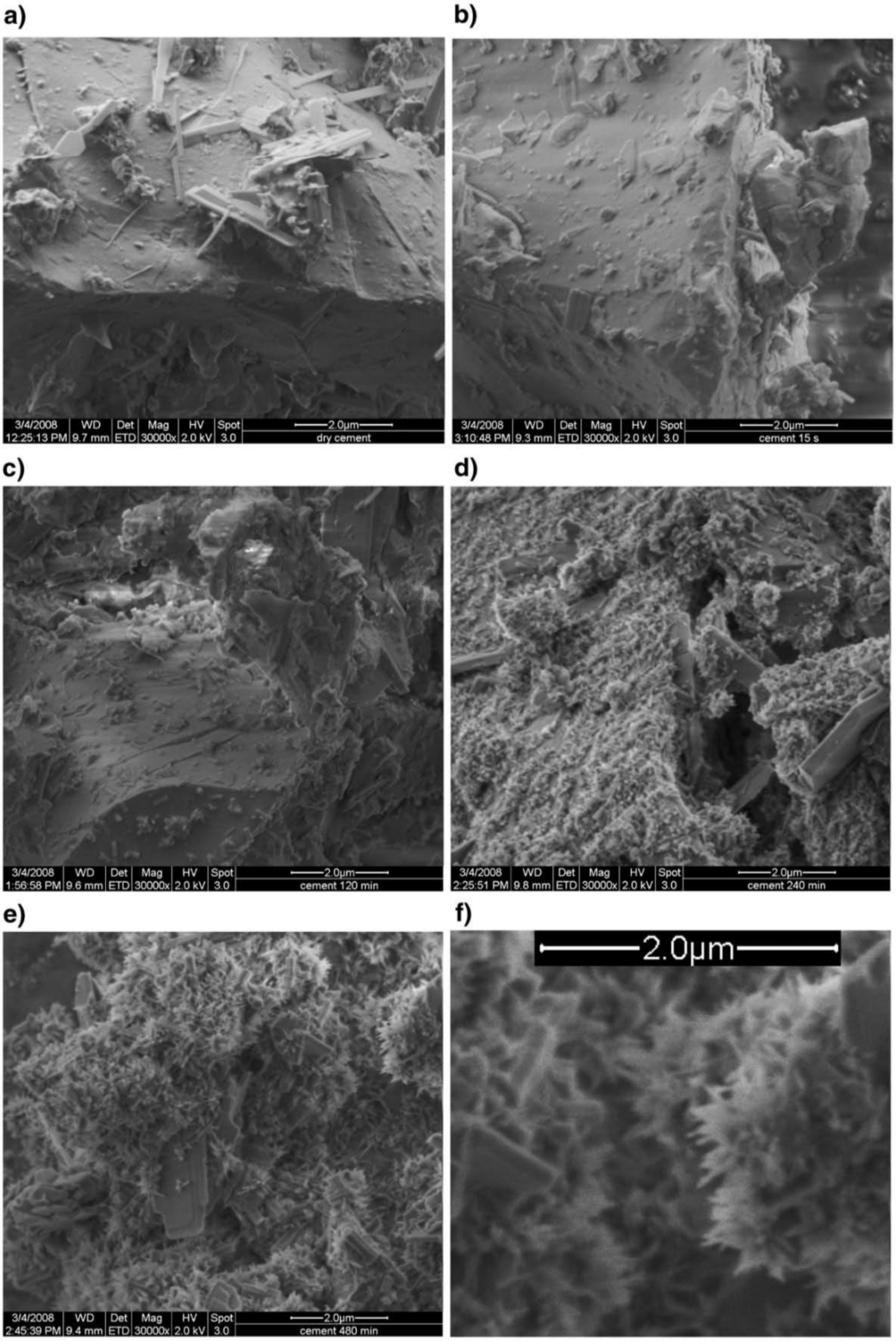

Figure 4.3 (Figure 8 in Paper II). SEM pictures of cement at different stages of hydration. a) Surface of unhydrated particle. b) Surface of particle hydrated for 15 s. c) surface of particle hydrated for 120 min. d) Surface of particle hydrated for 240 min. e) Surface of particle hydrated for 480 min. f) Surface of particle hydrated for 480 min at larger magnification.

4.1.3 Complementary observations by Isothermal Calorimetry and *ex situ* DR-FTIR (Paper III)

Isothermal calorimetry is a commonly used method to monitor the early hydration. Although it gives a good overview of the reaction process, the only information obtained is the flux of heat emitted at a given moment, which is the total heat of all reactions occurring at that instant. Reactions involving small enthalpy changes can be hard to discern, especially if reactions with high enthalpy changes are taking place simultaneously. In Paper III calorimetry showed that intensive mixing accelerated the hydration process (see Figure 4.4). This has been confirmed by later works done by others [40].

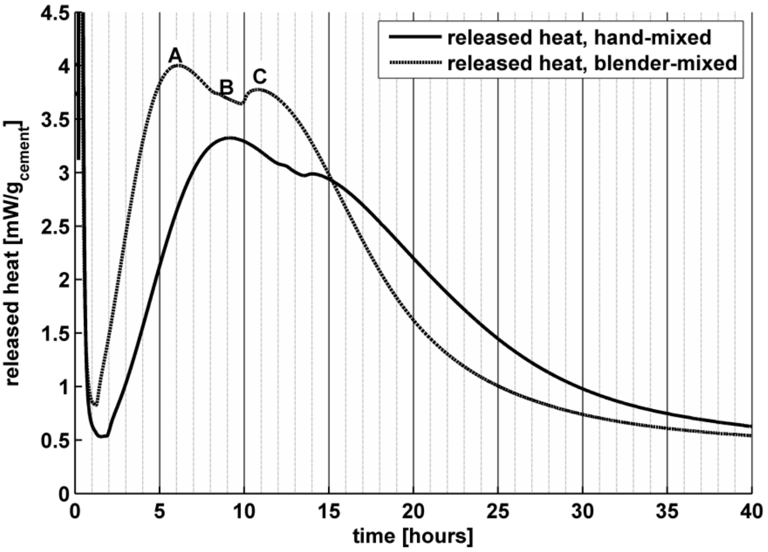

Figure 4.4 (Figure 1 in Paper III). Results from measurements with isothermal calorimetry on Portland limestone cement mortars made by hand mixing and mixed with a hand-blender.

Employing DR-FTIR in combination with freeze-drying as a complementary method to the isothermal calorimetry, changes in the latter was found to correlate with changes in the former. Moreover, utilizing corresponding IR fingerprints, it was found that the first peak, labelled A in Figure 4.4, is due to C-S-H formation, and that the subsequent peaks B and C are due to reactions involving sulfate transformations. The latter was identified as shifts in the sulfate regions (1100–1200 cm^{-1}) when the spectra taken before the calorimetry peaks was subtracted from the spectra taken after the peaks (marked with yellow in Figure 4.5).

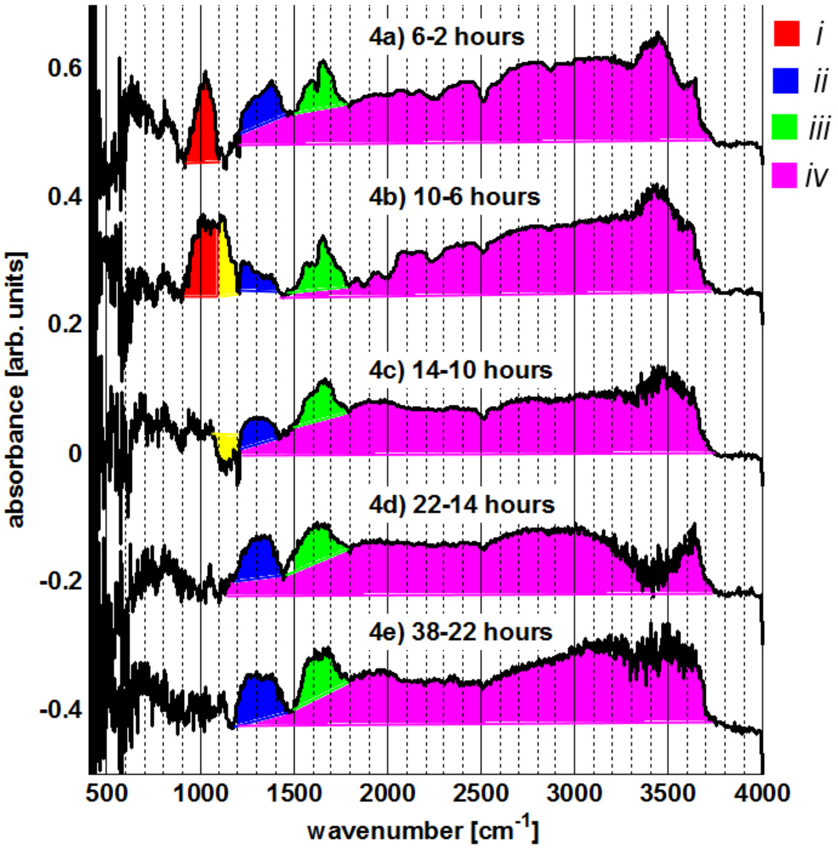

Figure 4.5 (Figure 4 in Paper III). The incremental, time resolved formations of hydration products in the hand-mixed mortar samples are reported, as seen by means of DR–FTIR difference spectra. Changes in products formed at different stages of hydration emerge by taking consecutive difference spectra. The spectra are deliberately offset to improve readability. The colours are only a guide for the eye. The signature of the transient compound is marked with yellow.

In the hardened concrete the monosulfates (AFm) may react with residual gypsum to form ettringite. The resulting volume expansion can cause cracks in the concrete and thus lower its strength. This is often referred to as delayed ettringite formation [41]. To prevent this, no more gypsum than necessary should be added to the concrete. The optimum amount corresponds to the case when all gypsum is consumed during the first day of hydration. However, it should be borne in mind that in cases when all gypsum is consumed there still remain transformations among the sulfate phases, which can be detected both with FTIR and isothermal calorimetry. These are further discussed in paper III. These transformations are delayed or do not occur if extra gypsum is added to the cement, as seen in Figure 4.6. The humps after the maximum of the main hydration peak are no longer present, giving the curve a smoother profile. This can be preferred if only the calcium silicate transformations are of interest.

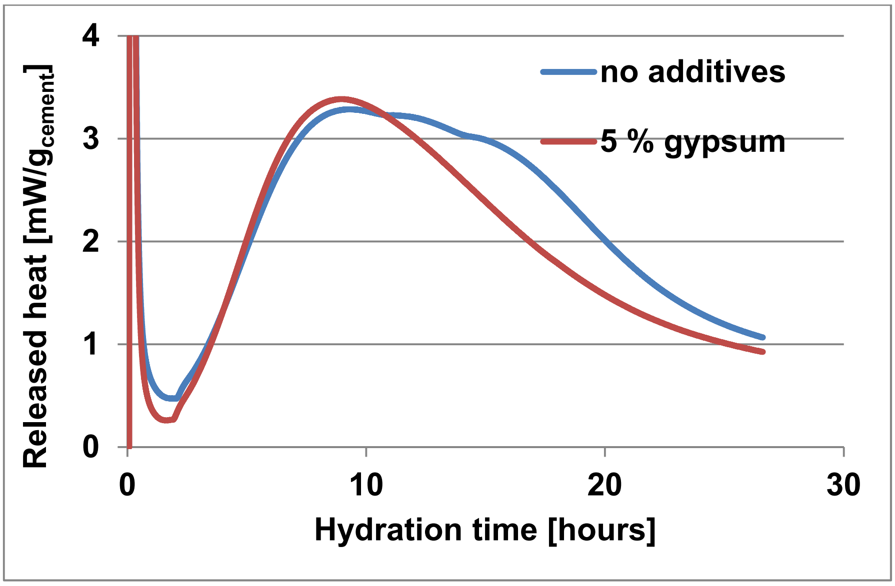

Figure 4.6. Measurements with isothermal calorimetry on Portland limestone cement illustrating the effect of adding 5 % additional gypsum.

4.2 Time Resolved Analysis of Cement Hydration by *in situ* ATR-FTIR Spectroscopy

4.2.1 Sample preparation for the ATR-FTIR analysis

Freeze-drying in combination with DR-FTIR has been shown to be a viable method to study the early hydration of Portland cement. However, even if freeze-drying is a gentle method to remove water, the removal of water from a wet system could affect its properties in a significant way. Although the methodology works for pure cement, it is expected that some additives could be more sensitive to the freeze-dry procedure, especially if they are distributed in liquid form. Also, the sampling is somewhat cumbersome since each sample must be handled separately, i.e. put in liquid nitrogen, ground after drying, placed in the sample cup of the spectrometer and then measured. Little effort is required for taking snap-shots at a few interesting points, but if series with closely spaced measuring points are needed the method becomes increasingly more labour intensive. *In situ* ATR (attenuated total reflection) FTIR was therefore employed and evaluated to complement the freeze-drying + DR-FTIR technique. To measure with ATR the cement paste sample was simply placed upon the internal reflection element (IRE) and pressed with a clamp against the IRE to maintain good contact to the IRE as the cement paste stiffens. The sample was also covered with a plastic lid to prevent it from drying owing to evaporation. Infrared spectra were then recorded automatically with predetermined intervals. As all the spectra were on the same sample, there was no need for a specific routine to obtain a good reference line for differential spectra (see Figure 4.7).

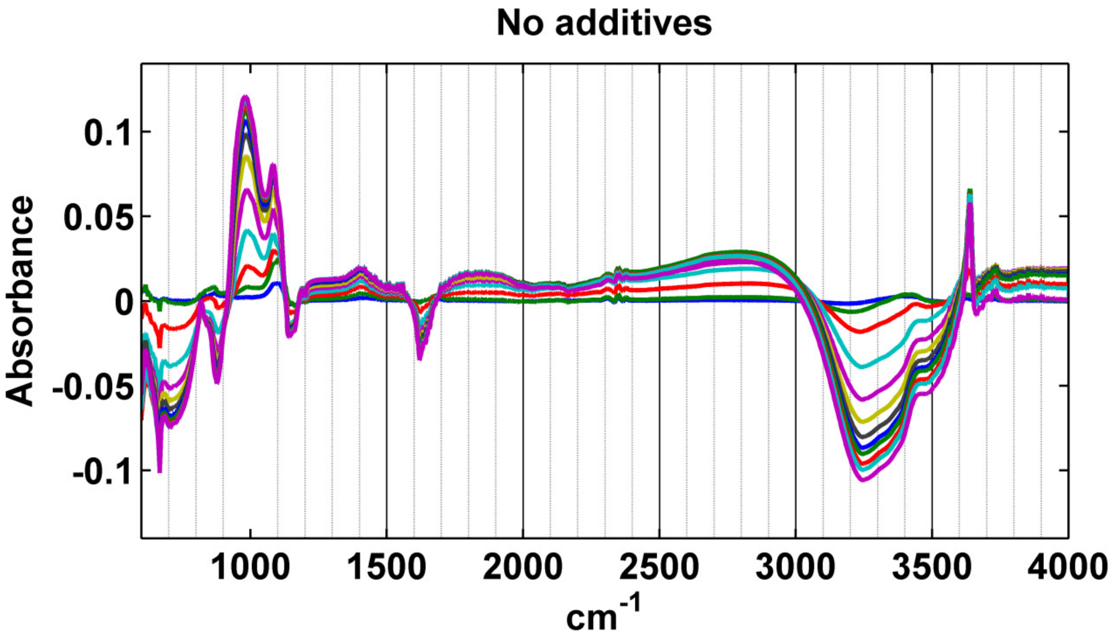

Figure 4.7 (from Figure 5 in Paper V). In-situ ATR difference spectra in the range 600–4000 cm^{-1} are displayed, acquired with 2 hours interval and arrived at after subtracting the raw spectrum acquired after 2 minutes.

4.2.2 Comparison between *ex situ* FTIR and *in situ* FTIR (Paper V)

Having the ability to measure cement hydration *in situ* gives the possibility to evaluate the effect of freeze-drying on the hydration products. However, there are some complications rendering a direct comparison difficult. One of them is that the *in situ* measurements contain liquid water, which has a strong infrared profile. This profile is absent in the freeze-dried samples, as the liquid water has been removed. A second complication has its origin in that during hydration an increased amount of water is incorporated into the hydration products. This water is not removed when the samples are freeze-dried. A consequence of this is that the amount of evaporated water will therefore affect the resulting molar concentrations of the other constituents. This dilution effect makes even inert phases, such as the limestone filler, appear to decrease. This is seen as dips in the carbonate absorption region (1400–1500 cm^{-1}). This is validated by the *in situ* measurements where the limestone concentration is constant and no dips appear.

This understanding was tested in Paper V. Thus, measurements on *ex situ* freeze-dried hydrated cement samples and *in situ* measurements on cement paste were performed by means of ATR in order to evaluate to what extent the freeze-drying methodology affects the chemical conclusions. Assuming the free water molecules in the samples to act as spectators, the spectral signature of liquid water was subtracted from both the DR-FTIR and the ATR spectra (having little effect on the freeze-dried samples for obvious reasons). Moreover, the spectra were scaled so that the area of the carbonate absorption was the same for all hydration times (having little effect on the *in situ* measurement for obvious reasons). This procedure allowed for a direct comparison between the two techniques (see Figure 4.8). The satisfactory agreement between the two techniques demonstrates the validity of the chemical insights gained from studies of freeze dried samples in previous works as well as the degree of transferability of spectral information after appropriate scaling.

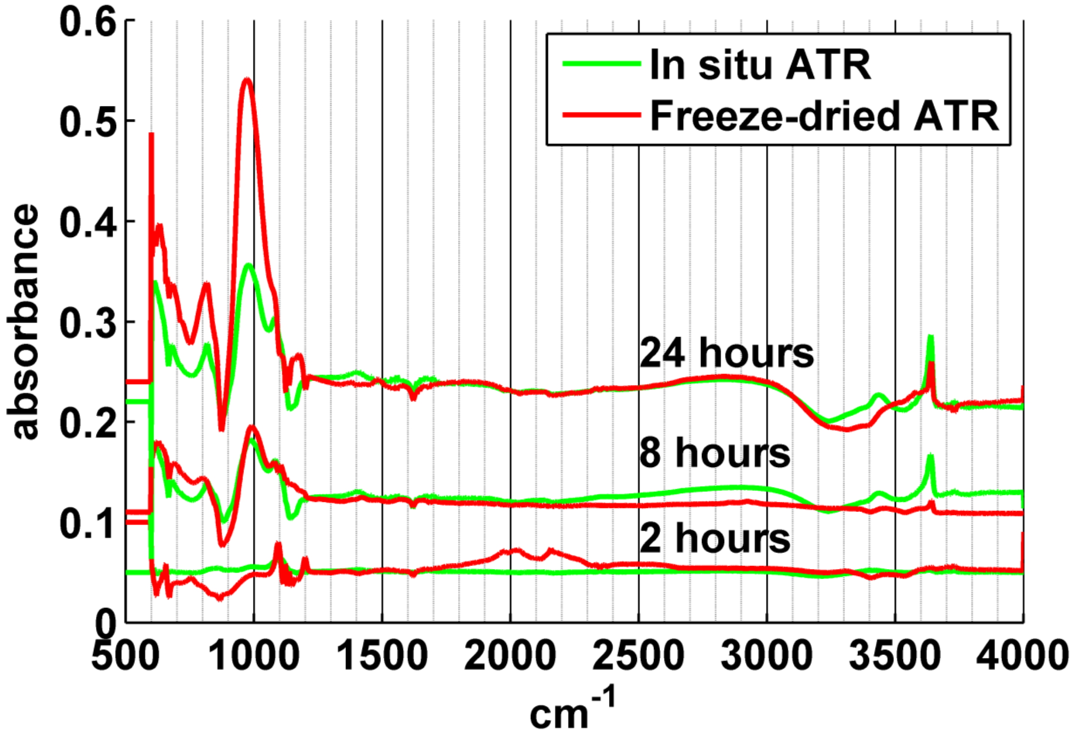

Figure 4.8 (Figure 3 in Paper V). Comparison between spectral information acquired *in situ* ATR and *ex situ* freeze-dry ATR demonstrating the degree of transferability of the two sample preparation techniques.

4.3 *In Situ* ATR and Isothermal Calorimetry (Paper V)

The possibility to acquire spectra automatically with any desired time intervals with *in situ* ATR greatly simplifies the comparison between IR and isothermal calorimetry. Thus, in Paper V this is done by monitoring the peak height at 980 cm^{-1}, corresponding to C-S-H, and differentiating it with respect to time. In Figure 4.9 the reactivity, as seen by IR, decreases significantly faster than what is observed by the calorimetry. This is not unexpected because the spectroscopic technique is biased to changes on clinker surfaces and at interfaces, and no spectroscopic changes are expected beyond the spectral saturations of these regions. This is in contrast to the calorimetry, which detects heat as long as chemical transformations occur. That the apparent delay of the calorimeter is caused by its thermal inertia is unlikely, as this effect would cause delays of the order of minutes [39]. The conclusion that the IR technique is mainly surface sensitive is consistent with the fact that the detection of initial hydration products by the spectroscopic method precedes that of the calorimetry. This is because initial surface hydration, while producing clear spectroscopic signatures, is associated with small heat fluxes.

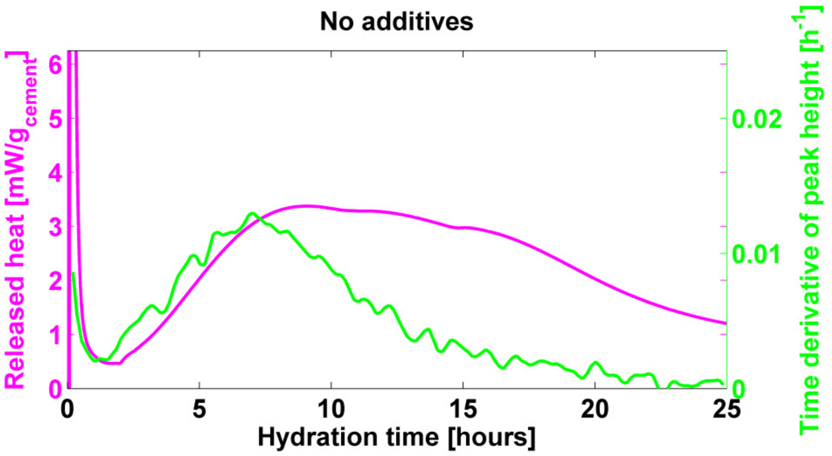

Figure 4.9 (Figure 6a in Paper V). Calorimetric data (purple) and the time derivative of the peak at 980 cm^{-1} (green) of cement paste without additives.

4.4 Application - Carbonation (Paper IV)

Cement hydration caused by air humidity is the main reason for aging of cement prior to its use. The susceptibility of clinker scale hydration to CO_2 in air would result in carbonate formation was the topic of paper (IV). Indeed, stopping the hydration with freeze-drying not only allows measurements on the cement at different stages of hydration, but also other means of testing can be performed. Thus, in Paper IV the hydration was stopped by freeze-drying at various times between 10 minutes and 8 hours. The samples were then exposed to carbonating atmosphere and the chemical transformations were followed with DR-FTIR. Figure 4.10 shows the result for the sample hydrated for 8 hours and subsequently exposed to normal atmospheric conditions. It was found that the hydration products were more susceptible to carbonation by integrating the carbonate region (marked as IV in Figure 2.1) in the FTIR spectra. Figure 4.11 shows that the longer the hydration, the faster the carbonation, at least for the early hydration.

Besides an ambient atmosphere, the carbonating atmosphere of pure humid CO_2 was tested. Here a separation of the C-S-H into calcium carbonate and silica was observed. The silica is seen as a peak at 1200 cm^{-1} Figure 4.12 (labelled III) and the breakdown is seen as a dip at 1000 cm^{-1} (labelled II) overlapping with the 1080 cm^{-1} peak of the calcium carbonate. The spectrum of calcium carbonate did not perfectly match any of the crystalline varieties. It also seemed to contain water. It was concluded that the carbonate was poorly crystalline or amorphous.

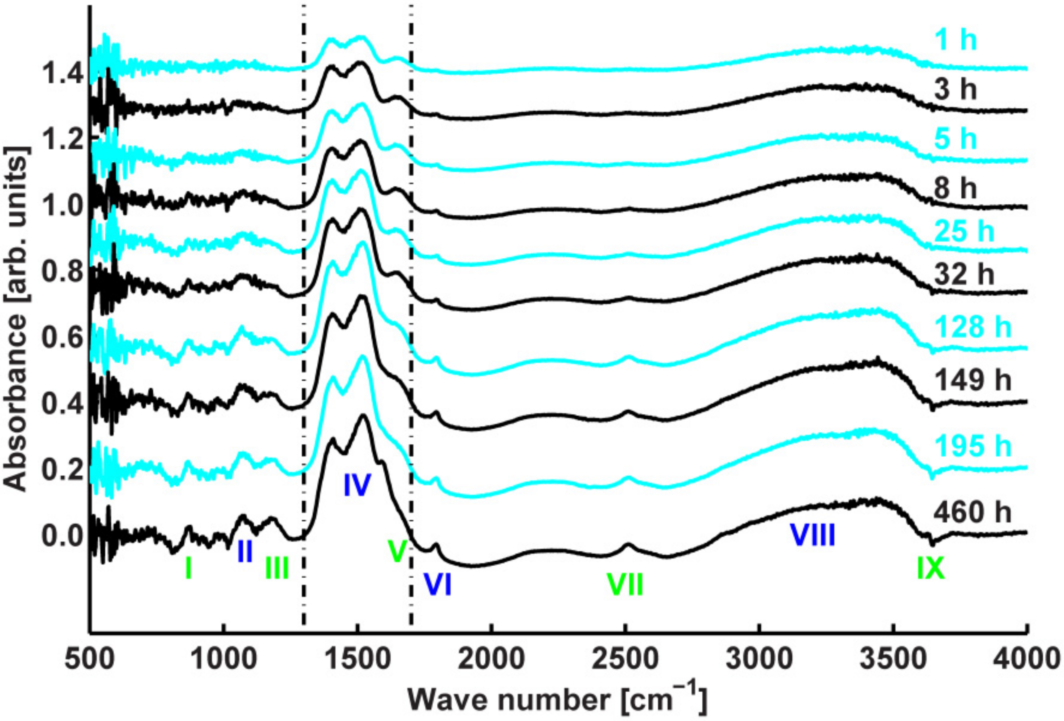

Figure 4.10 (Figure 2e in Paper IV). DR-FTIR spectra showing the effect of exposure to ambient air after selected time intervals samples hydrated for 8 h. The spectrum after 10 min of exposure was subtracted from all of the subsequent spectra to remove all signatures that are not the result of exposure.

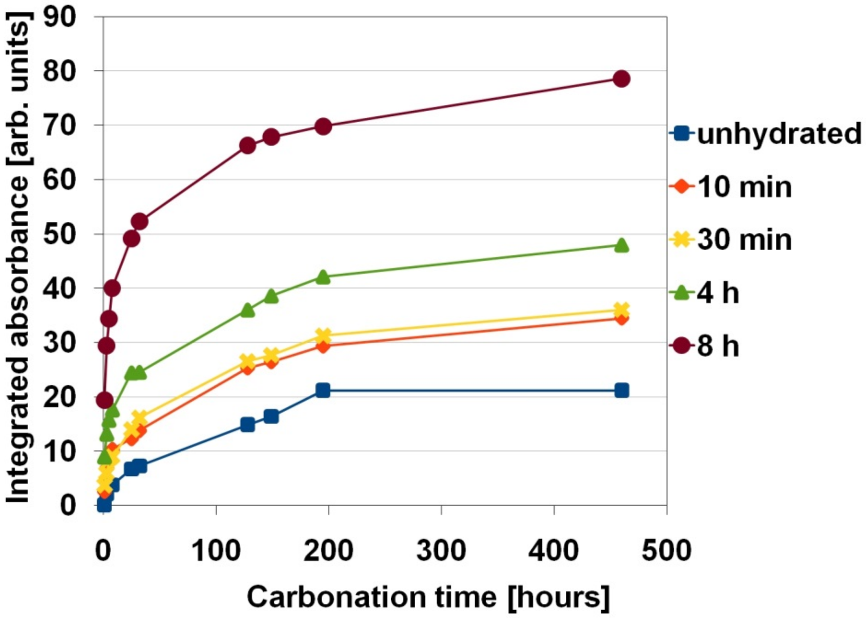

Figure 4.11 (Figure 3 in Paper IV). Integrated peak areas for unhydrated and hydrated samples exposed to ambient air as a function of exposure time. The integration range was 1300–1700 cm^{-1}, where the zero-level was set at 1300 cm^{-1}.The sample exposed for 10 min was used as reference for each hydration time.

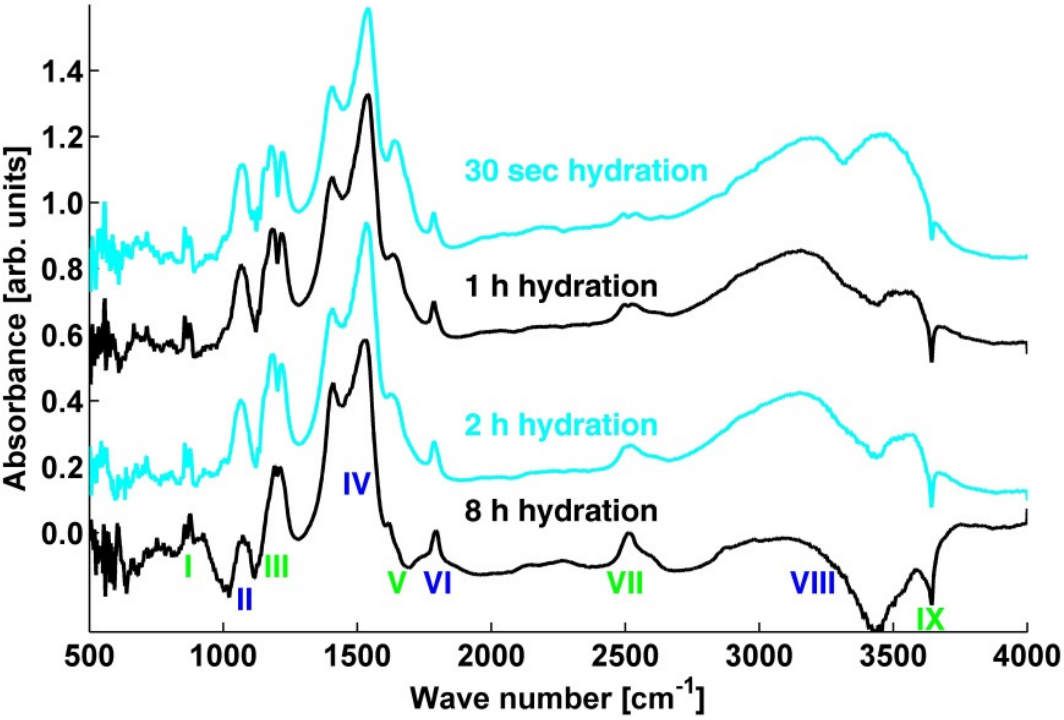

Figure 4.12 (Figure 6 in Paper IV).Enhanced DR-FTIR spectra showing the effect of exposure to a humid CO_2 atmosphere. The spectra of hydrated unexposed samples were subtracted from the spectra of the samples exposed to humid CO_2, cancelling the effect of hydration on the samples.

4.5 **Application - Accelerators (Paper I and Paper V)**

Accelerators are used to increase the reaction rate during the early hydration of cement. Colloidal nano-silica has been shown to have accelerating properties on Portland cement [27–29] (see also Figure 4.13).

CNS consists of silica networks and will therefore be visible at 1200 cm^{-1} in an FTIR spectrum. In Paper I freeze-drying was used together with DR-FTIR to follow CNS during hydration. By subtracting the spectra of cement paste without any admixtures from the spectra of cement paste containing CNS Figure 4.14 was obtained. It is seen that the silica particles are not completely dissolved in the alkaline conditions, but can be detected even after several days.

In Paper V the effect of CNS addition on Portland cement during early hydration was studied with *in situ* ATR and isothermal calorimetry. Figure 4.15 shows a comparison between the rate of formation of C-S-H and released heat. It is interesting to note that while the calorimetric data show little difference to the pure cement paste (Figure 4.9), the FTIR data shows a different profile. At the start of the main heat evolution peak the time derivative of C-S-H shows a shape that is more similar to the thermograms of cement paste with much higher amounts of CNS added, as seen in Figure 4.13. This observation emphasizes the conclusion previously drawn that the ATR spectra reflect surface processes. Thus, impact of CNS at clinker interfaces at early stages of hydration is clearly detected by the *in situ* ATR technique. Repeatedly, this is due to the sensitivity of ATR vibration spectroscopy to detect the surface chemistry, while isothermal calorimetry requires larger exothermal effects before the hydration can be detected.

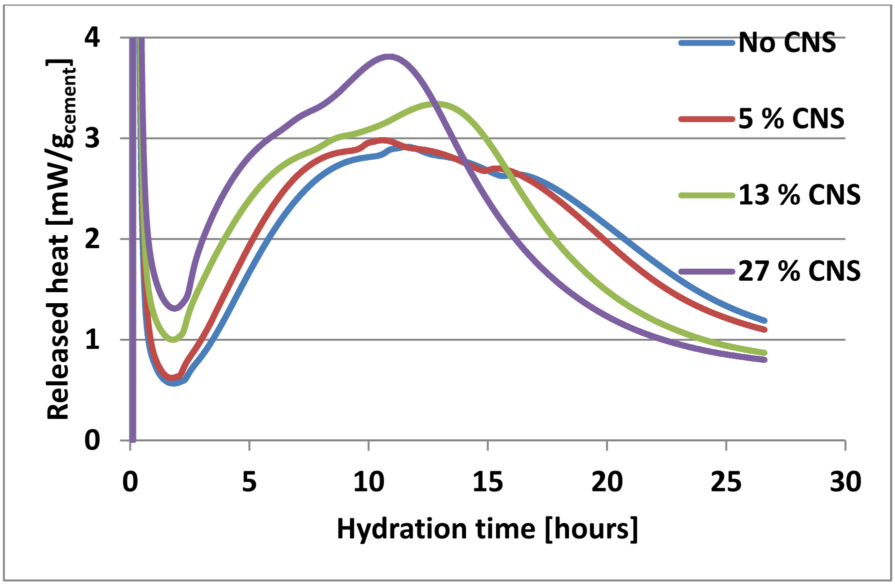

Figure 4.13. Results from measurements with isothermal calorimetry on Portland limestone cement with different amounts of CNS (Cembinder 50) added. The percentages are mass percentage of cement weight. The amount of water was adjusted such that all samples had a w/c ratio of 0.4.

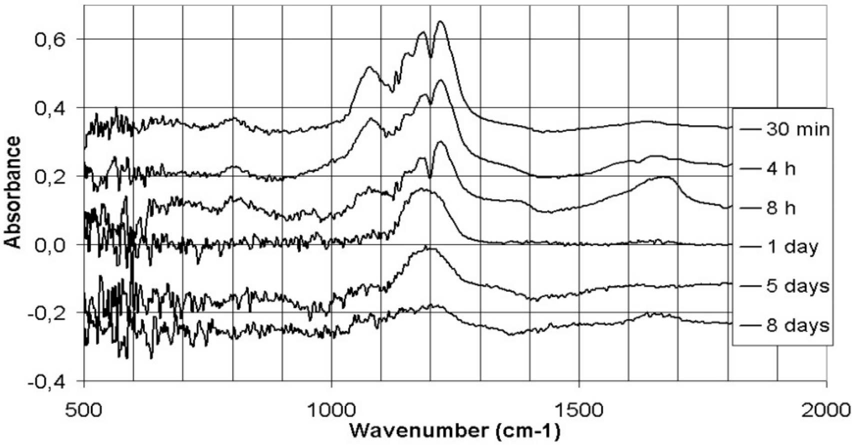

Figure 4.14 (Figure 6 in Paper 1). Difference spectra where spectra of cement paste with no additives have been subtracted from spectra of cement paste with 5 % Cembinder 8 added with the same hydration time. The times given to the right are the hydration times correlated to the spectra. The spectra are shown offset for clarity.

While acceleration of hydration is observed, the effect of CNS on the resulting hydration products seems to be small, as seen with FTIR (compare Figure 4.7 with Figure 4.16). This is not unexpected, partly because silica oligomerization is a main result of alite hydration, the difference being mainly quantitative. A second reason for the similarity is that because CNS hydrolysis is small during the first 24 h, the spectroscopic signatures of the CNS decomposition are equally small.

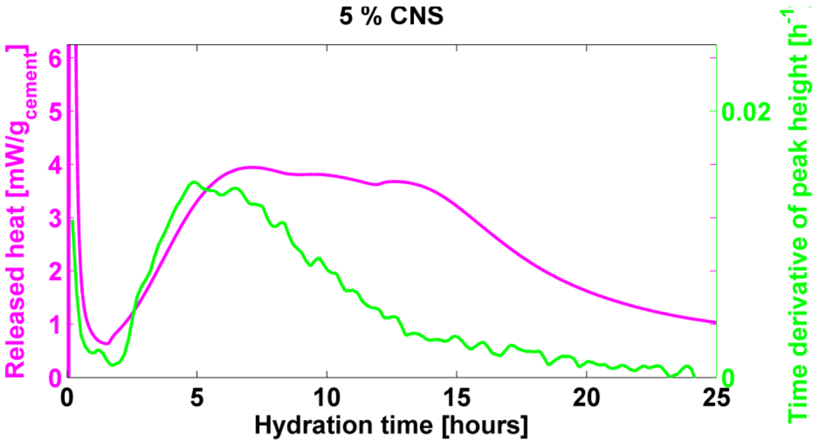

Figure 4.15 (Figure 6c in Paper V). Calorimetric data (purple) and the time derivative of the peak at 980 cm^{-1} (green) of after adding 5 wt % colloidal nano-silica (CNS).

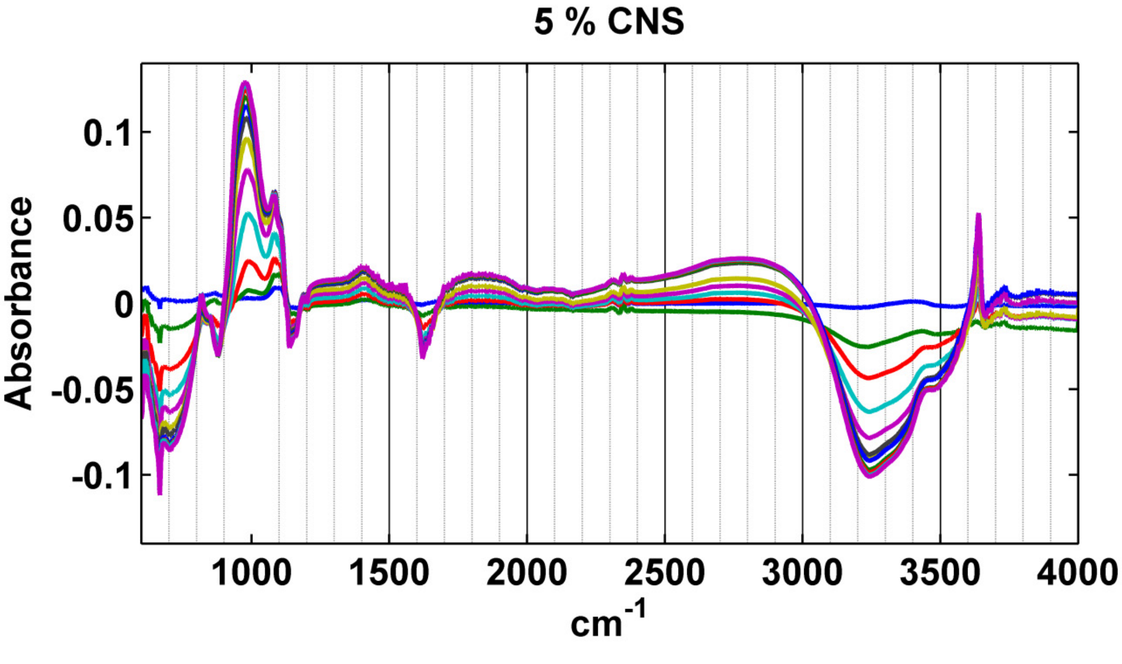

Figure 4.16 (from Figure 5 in Paper V). ***In situ*** **ATR difference spectra in the range 600–4000 cm^{-1} are displayed, acquired with 2 hours interval and arrived at after subtracting the raw spectrum acquired after 2 minutes after adding 5 wt % colloidal nano-silica (CNS).**

Taking the *in situ* ATR and isothermal calorimetry signatures of pure cement and CNS enhanced cement hydration as point of departures, two more accelerators were tested comprising sodium hydroxide and calcium chloride, respectively. Each significantly accelerates the rate of hydration of Portland cement, as seen in the thermograms in Figure 4.17.

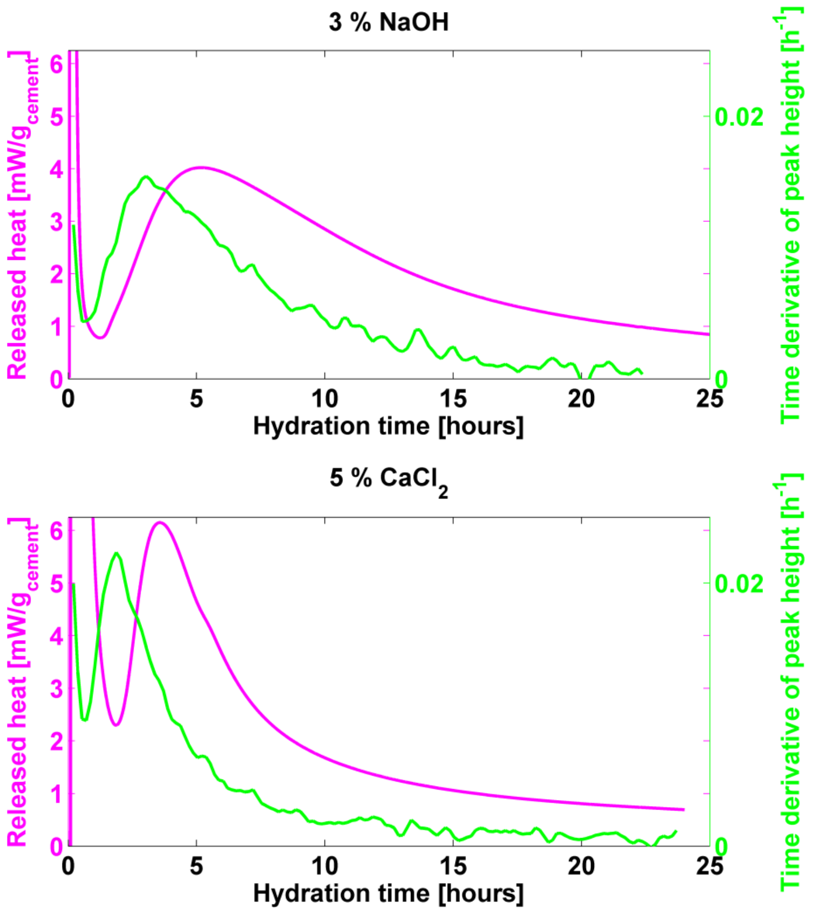
3 % NaOH

5 % $CaCl_2$

Figure 4.17 (Figure 6b and d in Paper V). Calorimetric data (purple) and the time derivative of the peak at 980 cm^{-1} (green) of after adding 3 wt % NaOH (top) and 5 wt% $CaCl_2$ (bottom).

The discrepancy between the calorimetry and *in situ* FTIR is here much more accentuated compared to the pure and CNS modified cement. This again underscores the observation that FTIR can give information not discernible with calorimetry. In particular, initial hydration involving the outer clinker scale, while causing chemical change upon C-S-H formation as seen by the infrared spectroscopy (see Figure 4.18), may not be related to detectable amounts of heat flux. By comparing the influences of the additives it is tempting to conclude that there is an initial excess of silica on the alite interfaces such that when dissolved calcium ions are added to the mortar rapid C-S-H formation is observed.

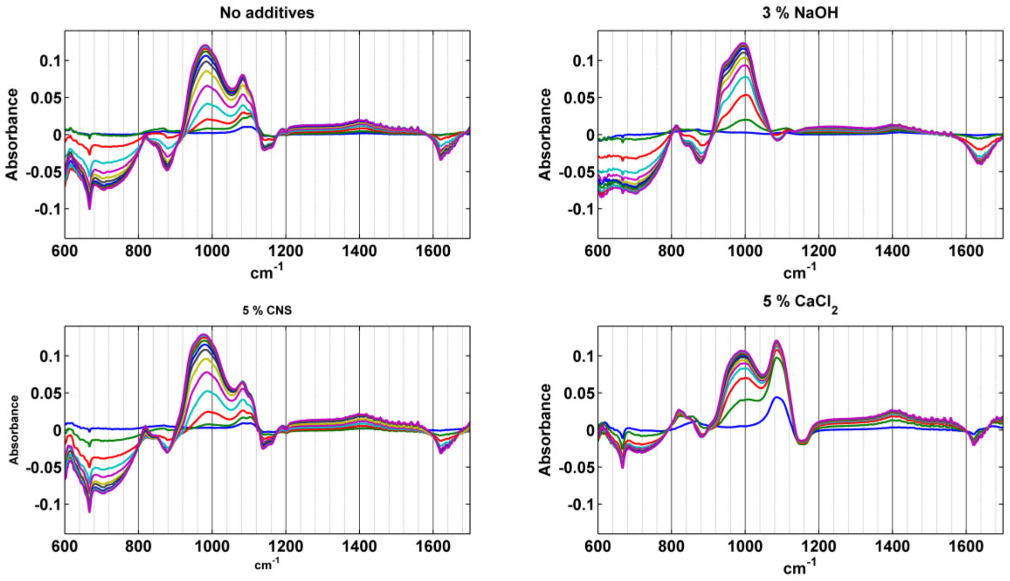

Figure 4.18 (Figure 5e-h from Paper V). ***In situ*** **ATR difference spectra in the range 600–1700 cm^{-1} are displayed, acquired with 2 hours interval and arrived at after subtracting the raw spectrum acquired after 2 minutes. (top left) no additives, (top right) after adding 3 wt% NaOH by cement weight, (bottom left) after adding 5 wt % colloidal nano-silica (CNS), (bottom right) adding 5 wt% $CaCl_2$.**

Finally, addition of CNS did not seem to affect the hydration products as compared to pure cement; this is apparently not the case for either NaOH or $CaCl_2$, as can be seen in Figure 4.18. In particular, their hydration profiles are markedly different from that of pure cement in the region 900–1200 cm^{-1}. Thus, although both accelerate the hydration and both form C-S-H, the resulting hydration compounds are distinctly different, and in particular so when comparing to pure cement. The results of papers I–III may be taken to suggest that they differ in the resulting C-S-H morphology.

5 Conclusions and Outlook

This work shows that diffuse reflection FTIR combined with freeze-drying provides an important complementary technique that contributes with essential aspects to the understanding of early cement hydration. Its strength rests in the fact that it provides global chemical information regarding the various types of bonding present in a sample. The fact that it is an *ex situ* technique, where the hydration is stopped at a chosen instance, allows for use of complementary methods on the same samples. Here, scanning electron microscopy was used to confirm that the chemical changes monitored with FTIR have corresponding changes occurring in the morphology. The time-resolution is satisfactory, as it is limited to the time it takes to freeze the sample, and the sample preparation is easy and gentle to the samples.

A complementary *in situ* measurement technique employing ATR-FTIR was developed and evaluated. Here the sample preparation is even simpler and non-invasive. The time resolution is still excellent, but with one major advantage: the spectra are acquired automatically with any desired time interval. Simply put the sample into the machine and collect the results the next day. The time-resolution is limited by the time it takes to acquire a spectrum; with the set-up used in this work a minute was enough to obtain good signal to noise ratio. In contrast, the *ex situ* technique requires that each sample is treated separately. Little effort is required for taking snap-shots at a few interesting points. However, if a series with closely spaced measuring points is needed then the method becomes increasingly more labour intensive. Having said this, by careful analysis consistency between the *ex situ* and *in situ* methodologies it was arrived at.

Ample amount of data generated with the *in situ* FTIR made is possible to make a more detailed comparison with isothermal calorimetry, another *in situ* technique with excellent time-resolution. By taking the peak height at 980 cm^{-1}, corresponding to C-S-H, and derivative with respect to time, a profile similar to the thermogram was obtained. However, there are discrepancies between the techniques: The thermogram reflects the heat evolution corresponding to complete hydration of the cement sample, while the *in situ* FTIR approach reports chemical transformations at clinker grains and interfaces. Evidently, the two techniques contribute useful complementary perspectives on the hydration process.

The simple sample preparation and use of FTIR, coupled with the quality of information obtained, should render its increased use for studying cement. The large amount of data might discourage new users unfamiliar with the technique. This work however, makes good use of difference spectra, where the non-changing contributions are subtracted. This simplifies the analysis and is strongly recommended if small changes in the spectra are sought.

This work has hydration of pure Portland cement paste as a main focus. The fact that FTIR can measure on any substance which contains infrared active groups makes it a suitable method for studying the effects of the increasing amounts of admixtures introduced into cements and mortars. This includes in principle all organic chemicals as well as a large portion of the inorganic additives. The impact of one such additive, i.e. colloidal nano-silica, on early cement hydration was addressed in present in this work. It was found that besides a slight acceleration of the hydration, the effect of CNS on the early hydration products was minor. This is in contrast to what is seen when adding CNS to the pure alite clinker phase, in case of which acceleration is indeed observed. The difference is owing to the complexity of the commercial product as compared to the pure synthetic model compound. In order to recover the inherent accelerating effect CNS on alite hydration, the passivating substances should be identified and tailored agents with high affinity to these substances introduced. The development of such chemical strategies is left for the future as are similar approaches to achieve novel energy efficient multifunctional building materials.

6 Acknowledgements

I would like to thank the following persons for contributing to my work:

My supervisors Itai Panas, Ulf Jäglid and Britt-Marie Steenari, who have given me so much support and knowledge with such enthusiasm.

Oliver Lindqvist and Jan-Erik Svensson for giving me the opportunity to work at Environmental Inorganic Chemistry.

The support from the Knowledge foundation (KK stiftelsen), the Swedish Research Council, and Eka Chemicals Inc., Bohus is gratefully acknowledged.

Inger Jansson and Lars Lindahl for valuable discussions and for providing me with the perspective of the industry.

Lars Wadsö, for making a specially designed calorimeter and letting us borrow it for free, and also for valuable help and discussions regarding calorimetry.

Kristian Larsson for helping me develop the DR-FTIR + freeze-drying technique.

Finally, I would like to thank my wife Anna. Her support was essential for this work.

7 References

[1] van Oss H. G., http://minerals.usgs.gov/minerals/pubs/commodity/cement/, January 2013 [Online] [Accessed 21 April 2013]
Available: http://minerals.usgs.gov/minerals/pubs/commodity/cement/mcs-2013-cemen.pdf.

[2] Taylor H. F. W., *Cement Chemistry*, Academic Press, London, 1992

[3] Malhotra V. M., *Global warming and sustainability issues as related to concrete technology*, Conference Proceedings for "International Symposium on Sustainability in the Cement and Concrete Industry" 17–26

[4] *Energiförsörjningen i Sverige*, Statens energimyndighet, 2008, ISSN 1403-1892

[5] J. S. Damtoft, *The sustainable cement production of the future,* Conference Proceedings for "International Symposium on Sustainability in the Cement and Concrete Industry" 75–84

[6] Bullard J. W., Jennings H. M., Livingston R. A., Nonat A., Scherer G. W., Schweitzer J. S., Scrivener K. L., Thomas J. J., *Mechanisms of cement hydration*, Cement and Concrete Research 41 (2011) 1208–1223

[7] Soper A.K., Benmore C. J., *Quantum Differences between Heavy and Light Water*, Physical Review Letters 101 (2008) 065502

[8] Noonan E. C., *Solubility of Salts in Deuterium Oxide*[1], Journal of the American Chemical Society 70 (1948) 2915–2918

[9] Tsurumi T., Hirano Y., Kato H, Kamiya T., Daimon M., *Crystal structure and hydration of belite*, Ceramic Transactions 40 (1994) 19–25

[10] Udagawa S., Urabe K., Natsume M., Yano T., *Refinement of the crystal structure of* γ-Ca_2SiO_4, Cement and Concrete Research 10 (1980) 139–144

[11] Iler R. K., *The Chemistry of Silica*, John Wiley & Sons, Inc., 1979, p 126

[12] Bonaccorsi E., Merlino S., Kampf A. R., *The Crystal Structure of Tobermorite 14 Å (Plombierite), a C–S–H Phase*, J. Am. Ceram. Soc., 88 (3) (2005) 505–512

[13] Bonaccorsi E., Merlino S., Taylor H.F.W., The crystal structure of jennite, $Ca_9Si_6O_{18}(OH)_6$•8H2O, Cement and Concrete Research 34 (2004) 1481–1488

[14] Mondal P., Jeffery J. W., *The crystal structure of tricalcium aluminate,* $Ca_3Al_2O_6$, Acta Cryst. B31 (1975) 689–697

[15] Bezou C., Nonat A., Mutin J.-C., Nørlund Christensen A., Lehmann M.S., *Investigation of the Crystal Structure of γ-CaSO4, CaSO4 · 0.5 H2O, and CaSO4 · 0.6 H2O by Powder Diffraction Methods*, Journal of Solid State Chemistry, 117 (1995) 165–176

[16] Hawthorne F. C., Ferguson R. B., *Anhydrous Sulphates II. Refinement of the Crystal Structure of Anhydrite*¸ Canadian Mineralogist 13 (1975) 289–292

[17] Hartman M R, Berliner R, *Investigation of the structure of ettringite by time-of-flight neutron powder diffraction techniques*, Cement and Concrete Research 36 (2006) 364 – 370

[18] Shivkumara C., Singh P., Gupta A., Hegde M.S., *Synthesis of vaterite* $CaCO_3$ *by direct precipitation using glycine and L-alanine as directing agents*, Materials Research Bulletin 41 (2006) 1455–1460.

[19] Clarkson J. R., Price T. J., Adams C. J., *Role of Metastable Phases in the Spontaneous Precipitation of Calcium Carbonate,* J. Chem. Soc. Faraday Trans. 88(2) (1992) 243–249.

[20] Xyla A. G., Koutsoukos P. G., *Quantitative Analysis of Calcium Carbonate Polymorphs by Infrared Spectroscopy*, J. Chem. Soc., Faraday Trans. 1 85(10) (1989) 3165–3172.

[21] Lam R. S., K., Charnock J.M., Lennie A., Meldrum F. C., *Synthesis-dependant structural variations in amorphous calcium carbonate*, CrystEngComm 9 (2007) 1226–1236

[22] Andersen F. A., Ljerka Brečević L., *Infrared Spectra of Amorphous and Crystalline Calcium Carbonate*, Acta Chemica Scandinavica 45 (1991) 1018–1024

[23] Coleyshaw E. E., Crump G., Griffith W. P., *Vibrational spectra of the hydrated carbonate minerals ikaite, monohydrocalcite, lansfordite and nesquehonite*, Spectrochimica Acta Part A 59 (2003) 2231–2239

[24] Graf D. L., *Crystallographic tables for the rhombohedral carbonates*, American Mineralogist 46 (1961) 1283-1316

[25] de Villiers J. P. R, *Crystal structures of aragonite, strontianite, and witherite*, American Mineralogist 56 (1971) 758-767

[26] Le Bail A., Ouhenia S., Chateigner D., *Microtwinning hypothesis for a more ordered vaterite model*, Powder Diffraction 26 (2011) 16-21

[27] Thomas J. J., Jennings H. M., Chen J. J., *Influence of Nucleation Seeding on the Hydration Mechanisms of Tricalcium Silicate and Cement*, J. Phys. Chem. C 113 (2009) 4327–4334

[28] Björnström J., Martinelli A., Matic A., Börjesson L., Panas I., *Accelerating effects of colloidal nano-silica for beneficial calcium-silicate-hydrate formation in cement*. Chemical Physics Letters 392(1-3) (2004) 242–248.

[29] Thomas J. J., Jennings H. M., Chen J. J., *Influence of Nucleation Seeding on the Hydration Mechanisms of Tricalcium Silicate and Cement,* J. Phys. Chem. C 113 (2009) 4327–4334

[30] Sadrmomtazi A., Fasihi A., *The Role of Nano-SiO2 Addition in the Mechanical Properties of RHA Composite Cement Mortars*, Advanced Materials Research 346 (2012) 18–25

[31] Aly M., Hashmi M.S.J., Olabi A.G., Messeiry M., Abadir E.F., Hussain A.I., *Effect of colloidal nano-silica on the mechanical and physical behaviour of waste-glass cement mortar,* Materials and Design 33 (2012) 127–135

[32] Shih J.-Y., Chang T.-P., Hsiao T.-C., *Effect of nanosilica on characterization of Portland cement composite*, Materials Science and Engineering A 424 (2006) 266–274

[33] Qing Y., Zenan Z., Deyu K., Rongshen C., *Influence of nano-SiO2 addition on properties of hardened cement paste as compared with silica fume,* Construction and Building Materials 21 (2007) 539–545

[34] Khaloo A. R., Vayghan A. G., Bolhasani M., *Mechanical and Microstructural Properties of Cement Paste Incorporating Nano Silica Particles with Various Specific Surface Areas,* Key Engineering Materials 478 (2011) 19–24

[35] Jalal M., Mansouri E., Sharifipour M., Pouladkhan A. R., *Mechanical, rheological, durability and microstructural properties of high performance self-compacting concrete containing SiO2 micro and nanoparticles,* Materials and Design 34 (2012) 389–400

[36] Gaitero J.J., Campillo I., Guerrero A., *Reduction of the calcium leaching rate of cement paste by addition of silica nanoparticles*, Cement and Concrete Research 38 (2008) 1112–1118

[37] Lothenbach B., Le Saout G., Haha M. B., Figi R., Wieland E., *Hydration of a low-alkali CEM III/B–SiO2 cement (LAC)*, Cement and Concrete Research 42 (2012) 410–423

[38] Griffiths P. R., de Haseth J. A., Fourier *Transform Infrared Spectrometry*, second ed., John Wiley & Sons, Inc., Hoboken, New Jersey, 2007

[39] Wadsö L., *Applications of an eight-channel isothermal conduction calorimeter for cement hydration studies,* Cement International, 3 (5) (2005) 94–101

[40] Juilland P., Kumar A., Gallucci E., Flatt R. J., Scrivener K. L., *Effect of mixing on the early hydration of alite and OPC system*, Cement and Concrete Research 42 (2012) 1175–1188

[41] Hewlett P. C., *Lea's Chemistry of Cement and Concrete*, fourth edition, Elsevier Ltd. 2008